

REPORT DOCUMENTATION PAGEForm Approved
OMB No. 0704-0188

The public reporting burden for this collection of information is estimated to average 1 hour per response, including the time for reviewing instructions, searching existing data sources, gathering and maintaining the data needed, and completing and reviewing the collection of information. Send comments regarding this burden estimate or any other aspect of this collection of information, including suggestions for reducing the burden, to the Department of Defense, Executive Service Directorate (0704-0188). Respondents should be aware that notwithstanding any other provision of law, no person shall be subject to any penalty for failing to comply with a collection of information if it does not display a currently valid OMB control number.

PLEASE DO NOT RETURN YOUR FORM TO THE ABOVE ORGANIZATION.

1. REPORT DATE (DD-MM-YYYY) 01-08-2012	2. REPORT TYPE Master's Thesis	3. DATES COVERED (From - To) FEB 2012 - AUG 2012	
4. TITLE AND SUBTITLE MICROENCAPSULATION OF SELF-HEALING CONCRETE PROPERTIES		5a. CONTRACT NUMBER N00244-10-G-0004	
		5b. GRANT NUMBER	
		5c. PROGRAM ELEMENT NUMBER	
6. AUTHOR(S) James Gilford III		5d. PROJECT NUMBER	
		5e. TASK NUMBER	
		5f. WORK UNIT NUMBER	
7. PERFORMING ORGANIZATION NAME(S) AND ADDRESS(ES) Louisiana State University			
8. PERFORMING ORGANIZATION REPORT NUMBER			
9. SPONSORING/MONITORING AGENCY NAME(S) AND ADDRESS(ES) Naval Postgraduate School Monterey, CA 93943			
10. SPONSOR/MONITOR'S ACRONYM(S) NPS			
11. SPONSOR/MONITOR'S REPORT NUMBER(S)			
12. DISTRIBUTION/AVAILABILITY STATEMENT 1. DISTRIBUTION STATEMENT A. Approved for public release; distribution is unlimited.			
13. SUPPLEMENTARY NOTES			
14. ABSTRACT Recent studies in the literature have demonstrated the ability of self-healing processes to be effective in enhancing the overall life of concrete. The main goal of this project is to evaluate and to control specific parameters for the production of an effective self-healing matrix that can be utilized within the application of self-healing concrete. Therefore, the project objective is to synthesize microcapsules using dicyclopentadiene and sodium silicate and to evaluate the effects of pH, temperature, and agitation rate on microcapsule morphology. The microcapsule diameter, yield analysis, and shell thickness were characterized using scanning electron microscopy. During the experimental analysis, it was determined that temperature possesses a direct relationship with the pH for both sodium silicate and DCDP. As the temperature increased during the trials, the pH decreased. Temperature had a direct impact on the forming of the wall and core during the interfacial polymerization phase. Although the ability to maintain this consistency with the pH is important and essential, agitation rate is the key factor that controls the microcapsule capsule diameter size. As the agitation rate is increased, the microcapsule diameter size will decrease. If the agitation rate decreases, the microcapsules will become larger.			
15. SUBJECT TERMS			
16. SECURITY CLASSIFICATION OF: a. REPORT	17. LIMITATION OF ABSTRACT UU	18. NUMBER OF PAGES 99	19a. NAME OF RESPONSIBLE PERSON Julie Zack, Educational Technician
b. ABSTRACT	c. THIS PAGE		19b. TELEPHONE NUMBER (Include area code) (831) 656-2319

Reset

Standard Form 298 (Rev. 8/98)

Prescribed by ANSI Std. Z39-18

Adobe Professional 7.0

MICROENCAPSULATION OF SELF-HEALING CONCRETE PROPERTIES

A Thesis

Submitted to the Graduate Faculty of the
Louisiana State University and
Agricultural and Mechanical College
in partial fulfillment of the
Requirements for the degree of
Master of Science

in

The Interdepartmental Program in Engineering Science

by
James Gilford III
B.S., Prairie View A&M University, 2001
August 2012

ACKNOWLEDGEMENTS

This thesis project would not have been possible without the support of many people. The author would first like to express his gratitude to his major professor, Dr. Marwa Hassan, for the opportunity she provided in conducting this research. Her support, guidance and encouragement were invaluable throughout the journey. The author is also thankful for the assistance and knowledge provided by the supervisory committee members, Dr. Michele Barbato and Dr. Ayman Okeil. Further, the author would like to extend his gratitude to the Department of Construction Management and Industrial Engineering, and the United States Navy for financial assistance.

A special thanks is also given to all his colleagues, Heather Dylla and Megan Hurst for laboratory assistance. A special thanks is given to James and Gwendolyn Gilford, Jr., Katelyn T. Gilford and Cleve and Adele Glenn for their support throughout my endeavors. Lastly, the author would like to thank all of my extended family and friends who supported me until the end.

THANK YOU!

TABLE OF CONTENTS

ACKNOWLEDGEMENTS	ii
ABSTRACT	v
CHAPTER 1	1
INTRODUCTION	1
1.1 Problem Statement	1
1.2 Objectives	2
1.3 Research Approach	2
1.4 References	3
CHAPTER 2	4
LITERATURE REVIEW	4
2.1 Concrete Self-Healing Methods	4
2.1.1 Overview of Self-Healing Processes and UF Resins	4
2.1.2 Hollow-Fiber Glass Systems	5
2.1.3 Autonomic Healing of Polymer Composites	6
2.2 Microcapsule Synthesis	7
2.2.1 Micro-Encapsulation Processes	8
2.2.2 Effect of Temperature	9
2.2.3 Effect of RPM and Droplet Size	10
2.3 Characterization of Microcapsules	10
2.3.1 Transmission Electron Microscopy Analysis	10
2.3.2 Atomic Probe Microscopy	11
2.3.3 SEM Analysis	12
2.3.4 SEM Procedures and Imagery Analysis	14
2.4 References	19
CHAPTER 3	22
MICRO-ENCAPSULATION OF SELF-HEALING CONCRETE PROPERTIES	22
3.1 Introduction	22
3.2 Background	23
3.2.1 Overview of Self-Healing Methods	23
3.2.2 Microencapsulation Procedures	25
3.3 Experimental Program	26

3.3.1 Materials	26
3.3.2 Equipment	27
3.3.3 DCDP Micro-Encapsulation Procedures	27
3.3.4 Sodium Silicate Microencapsulation	29
3.4 Results and Analysis	31
3.4.1 Microcapsule Parameter Analysis.....	31
3.4.2 Microcapsule Morphology and Shell Thickness.....	31
3.4.3 Controlling Diameter and Size.....	36
3.5 Conclusions.....	38
3.6 References.....	39
CHAPTER 4	41
SUMMARY AND CONCLUSIONS	41
4.1 Future Work	41
Appendix: SEM MICROCAPSULE ANALYSIS.....	42
VITA	48

ABSTRACT

Recent studies in the literature have demonstrated the ability of self-healing processes to be effective in enhancing the overall life of concrete. The main goal of this project is to evaluate and to control specific parameters for the production of an effective self-healing matrix that can be utilized within the application of self-healing concrete. Therefore, the project objective is to synthesize microcapsules using dicyclopentadiene and sodium silicate and to evaluate the effects of pH, temperature, and agitation rate on microcapsule morphology. The microcapsule diameter, yield analysis, and shell thickness were characterized using scanning electron microscopy. During the experimental analysis, it was determined that temperature possesses a direct relationship with the pH for both sodium silicate and DCDP. As the temperature increased during the trials, the pH decreased. Temperature had a direct impact on the forming of the wall and core during the interfacial polymerization phase. Although the ability to maintain this consistency with the pH is important and essential, agitation rate is the key factor that controls the microcapsule capsule diameter size. As the agitation rate is increased, the microcapsule diameter size will decrease. If the agitation rate decreases, the microcapsules will become larger. Sodium silicate, however, was not consistent with the normal parameter matrix, due to its alkaline nature. As the agitation rate increased, the size remained normal and consistent. This was due to the attempt to stabilize the sodium silicate solution for the micro-encapsulation procedure of Urea-Formaldehyde. Nevertheless, both sodium silicate and DCDP trials were successful in meeting the overall objective of this thesis, which was to control the performance parameters of the two self-healing methods.

CHAPTER 1

INTRODUCTION

Concrete is exposed to external factors such as extreme heat, cold, stress, during service. Concrete shrinks and expands with variations in moisture and temperature. Cracks can occur when changes to accommodate these factors are not implemented in the design and development. Other factors that can affect concrete and its lifespan include shrinkage, design flaws or poor quality of construction materials (Mather 1989). Concrete experiences various loading from heavy vehicles, earthquakes and strong winds. Due to these factors in addition to several more it is inevitable that reinforced concrete eventually develop cracks. When cracks originate in concrete structures, a sequence of serious events begins to occur within those structures. Not only do these cracks affect the functionality of the structure, but they also affect the durability and strength of the structure. In order to enhance concrete resistance to these defects and degradations, the innovation of self-healing concrete is promising.

Self-healing concrete can be defined as concrete that possesses self-healing agents, which will ‘automatically heal’ concrete structures, when cracks occur during their life cycle. Self-healing agents may be transferred through strong core microcapsules, hollow reinforced fibers and even by forms of organic matter (Ming Qiu Zhang et al 2011). All of these methods are currently undergoing testing and analysis in order to test their durability and longevity. This research deals with a number of self-healing chemicals that are used in the micro-encapsulation process.

1.1 PROBLEM STATEMENT

Recent studies in the literature have demonstrated the ability of self-healing processes to be effective in enhancing the overall life of concrete (Keesler et al. 2003). Although, the application of this technology and recent innovation is still in its experimental phases, its contributions towards effectively healing concrete possess outstanding possibilities. Therefore, there are many future environmental designs and operational factors that still need to be assessed. Factors that control the morphology, shell thickness and strength of these capsules have not been thoroughly tested.

1.2 OBJECTIVES

To address the aforementioned problem statement, the main goal of this project is to evaluate and to control specific parameters for the production of an effective self-healing matrix that can be utilized within the application of self-healing concrete. The healing process that has been chosen for this analysis is that of self-healing by microencapsulation. To achieve this goal, this study met the following objectives:

1. Synthesize microcapsules using Dicyclopentadiene (DCDP) and Sodium Silicate;
2. Evaluate the effects of pH, temperature, and agitation rate on microcapsule morphology (diameter, shell thickness, shape);
3. Evaluate Yield

1.3 RESEARCH APPROACH

To achieve the aforementioned objectives, this study was divided into four phases comprised of the following nine tasks:

Phase 1: Manufacturing of Microcapsules

Task 1: Purchase appropriate equipment to manufacture microcapsules

Task 2: Implement urea-formaldehyde procedures to produce DCDP microcapsules

Task 3: Implement urea-formaldehyde procedures to produce sodium silicate

Phase 2: Evaluate the effect of PH on the microcapsules synthesized

Task 4: Synthesize microcapsules using the DCDP and sodium silicate methods developed in Phase 1 with various pH levels

Task 5: Characterize resulting microcapsules' diameter, morphology, and shell thickness using Scanning Electron Microscopy (SEM)

Phase 3: Evaluate the effect of Temperature on the microcapsules synthesized

Task 6: Synthesize microcapsules using the DCDP and Sodium Silicate methods developed in phase 1 with various temperature levels

Task 7: Characterize resulting microcapsules' diameter, morphology, and shell thickness

Phase 4: Evaluate the effect of the agitation rate on the microcapsules synthesized

Task 8: Synthesize microcapsules using the DCDP and sodium silicate methods developed in Phase 1 with various agitation rates

Task 9: Characterize resulting microcapsules' diameter, morphology, and shell thickness

1.4 REFERENCES

Concrete Technology, Past, Present and Future, Proc. Of V. MOHAN Malhotra Symposium, ed. By P.K. Mehta, ACI SP-144, 1-30, (1994).

Darter, M. Abdelrahman, M., Okamoto, P., and Smith, D. Performance Related Specifications for Concrete Pavements. FHWA-RD-93-042. Federal Highway Administration, Washington, D.C, 1993.

Mather, B. How to Make Concrete That Will Be Immune to the Effects of Freezing and Thawing. Performance of Concrete, American Concrete Institute, Vol. 122, 1989, pp. 1-18.

Ming Qiu Zhang, Min Zhi Rong. *Self-Healing Polymers and Polymer Composites*, First Edition. © 2011 John Wiley & Sons, Inc. Published 2011 by John Wiley & Sons, Inc.

Kessler, M.R., N.R. Sottos, and S.R. White. "Self-healing Structural Composite Materials." *Composites Part A: Applied Science and Manufacturing* 34.8 (2003): 743-53.

CHAPTER 2

LITERATURE REVIEW

2.1 CONCRETE SELF-HEALING METHODS

There are various self-healing methods for concrete that have been instituted throughout modern practices. Some of these methods consist of the following: Hollow Fiber Glass Systems, Autonomic Healing of Polymer Composites, and Microencapsulation of Self-Healing Agents. In the following sections, a detailed and thorough overview is provided concerning these processes and methods.

2.1.1 Overview of Self-Healing Processes and UF Resins

During service, concrete is exposed to multiple external factors such as extreme heat, cold, and stresses. Due to these external factors, as well as possible shrinkage, design flaws or poor quality of construction materials, reinforced concrete will eventually develop cracks. Inevitable damage to concrete structures occurs by cracks originating in these structures by steel oxidation, resulting in strength loss for reinforced concrete structures (Schlangen, E. 2005). Not only do these cracks adversely affect the many components within the structure, but they also reduce the durability and strength of the structure. Self-healing concrete components assist in remedying this dynamic event.

Numerous methods and processes are available for self-healing cracks within damaged concrete. The methods include, but are not limited to, natural healing, autonomic healing, activated processes, autogeneous healing, etc. Natural healing occurs when a concrete crack is automatically and naturally blocked without use of a chemical matrix or design. The autonomic healing process is a method that utilizes a ‘specialized design matrix’ of specific man made materials to aid in the healing process. These materials assist in sealing the crack within in an expedited manner. The activated process utilizes a different mechanism, which is previously implemented and placed in the concrete beforehand. Autogeneous, which means produced from within or self-generating incorporates not only natural healing, but the autonomic process (self-managing) as well. Although these methods are reliable and consistent, crack propagation plays a large role on its healing effectiveness.

There are a multitude of methods that exist, which can incorporate and utilize the different self-healing methods and mechanisms. A method that incorporates autogeneous, autonomic and the activated methods is the method of U-F (Urea-Formaldehyde). Urea-Formaldehyde resin, which was discovered between 1800 – 1885, implements a reaction of urea and formaldehyde, which produces a resinous material (Rammon et al. 1986). A large amount of urea-formaldehyde is produced each year by industry. This polymethylene resin is mostly used in bonding particle board, hardwood plywood and laminating adhesive. Some of the properties of this chemical includes a high surface hardness, volumetric resistance, and high tensile strength.

There are two different developments for the synthesis of Urea Formaldehyde. The first is incorporated and conducted at an alkaline pH (normally using an alkaline catalyst and ammonia) which produces a methylol urea. The second uses an acid pH, which results in the strengthening of methylol and forms a polymeric material (Rammon et al. 1986). The solid formation of material during the aqueous phase after the polymerization of urea and formaldehyde is due to the high molecular weight polymers (Dunker et al. 1986).

2.1.2 Hollow-Fiber Glass Systems

FRP's (Fiber-Reinforced Polymer's) have great performance characteristics in relation to strength and stiffness. FRP's allow for a versatility and flexibility in performance. Nevertheless, due to their inherent micro-structure, delamination may occur due to its poor performance under loading (Kessler et al. 2002). FRPs not only give an advantage to incorporate a healing agent, but they also have positive structural improvements. When failure or overstresses of broken fibers occur, the healing agents flow into the damaged area. Some chemicals used in the past for healing agents are ethyl cyanoacrylate, methyl methacrylate, and cyanoacrylate (Kessler 2002).

Glass fibers, which contain specific healing agents, can represent two different methods. One method can serve as a one-part adhesive, such as cyanoacrylate. The system can also serve as a two-part epoxy system, containing both a resin and a hardener. Both of these methods will be located perpendicular to one another; however, one is implemented within the matrix itself and one within the fibers (Kessler 2002). It has been shown in previous studies that these hollow fibers are multifunctional; since the fibers themselves store a liquid healing agent while simultaneously provide structural reinforcement.

These hollow fiber systems offer a flexibility to place healing plies in different locations within the laminate in order to tailor the repair to the likely damage. This is an excellent process for the self-healing of concrete process. However, if these self-healing hollow glass fibers are not located in an area where the crack occurs, the self-healing agent will not be utilized. Although an excellent method, more research and analysis must be completed before implementation into the market place.

2.1.3 Autonomic Healing of Polymer Composites

As previously discussed and addressed with Hollow Glass Fiber Healing, it was founded that cracks can develop deep within polymer structures, causing mechanical degradation at times. Despite the bases for the cracks, the composition of the polymer structure can be significantly compromised (Wool 1995). Beyond the Hollow Glass Fiber method, an additional process exists in which a structural polymeric material has the capability to automatically heal cracks within concrete structures. Just like the Hollow Glass Fiber Self-Healing method, a microencapsulated healing agent is released into the crack plane once the damage occurs. Once the healing agent comes into contact with the embedded catalyst, a bonding action takes place called Polymerization (Lee 1991). Autonomic healing consists of polymerization capsules that have non-ending chain ends. This allows the epoxy matrix to heal multiple cracks simultaneously (Zihlif et al. 2011).

Regardless of the application or design of the microcapsule, configuration and geometry is the key. The walls on the manufactured capsules cannot be too profuse or too small; otherwise, they might rupture prematurely or might not rupture at all (Dry 1996). An additional and important design factor is the microcapsules' strength and stiffness as well as the relationship between the microcapsules and the matrix. This supports a theory known as ROMP (ring opening metathesis polymerization). There are several essential factors that have contributed to the ROMP theory (Dry and Sottos 1993). These factors are as follows:

1. Promotes long life
2. Low monomer viscosity
3. Rapid polymerization at ambient conditions
4. Low shrinkage upon polymerization

This linked polymer network causes a reaction that polymerizes dicyclopentadiene (DCDP) at room temperature within minutes (White et al. 2001). DCPD, a highly stable monomer with excellent shelf life, was encapsulated in urea formaldehyde (UF) microcapsules. These DCDP micro-capsules (filled with urea-formaldehyde) provide a protective shell between the catalyst and the DCDP in order to prevent premature polymerization during the development of the composite (Brown et al. 2003). In order to ensure that polymerization has occurred, SEM and microscopy analysis were administered on the specimens. Effectiveness of the healing agent was shown by damage under the SEM, as well as absorption within the film through Infrared Spectroscopy.

Materials and components such as these presented should increase the reliability and service life of thermosetting polymers (Brown et al. 2003). However, the amount utilized when placing DCDP microcapsules within concrete structures is unclear. In addition, there are many questions that must and should be answered in order to effectively utilize this unique and rare self-healing property in the commercial market. For example, the reproduction potential in mass quantity is speculative.

2.2 MICROCAPSULE SYNTHESIS

This section and Figure 2.1 explains the sequence of events that take place during the development of microcapsule formation and generation. Section A is a representation of the ingredients and additives with H₂O. These additives are mixed together with a stirring device in order to create an emulsion. Section B is a representation of an agent separating themselves from the emulsion. Section C is an illustration of the healing agent being encapsulated by the surfactant being utilized. Section D is the final result of the microcapsule itself with the healing agent stabilized inside. This basic process is the end result of the entire microencapsulation process itself. The objective of these steps is to streamline the process using different chemicals, techniques, and procedures.

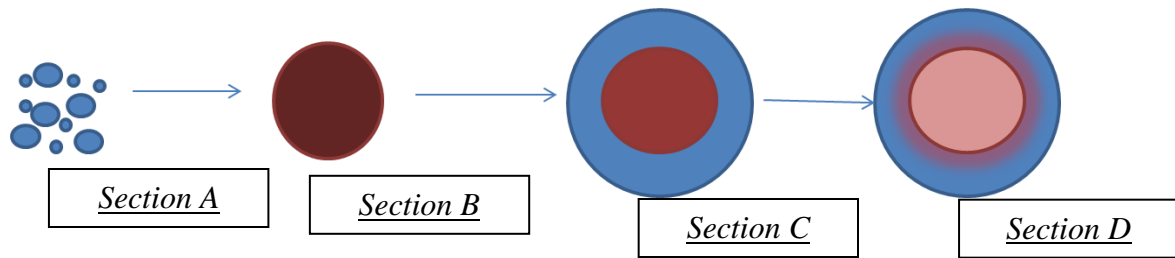


Figure 2.1 Microcapsule Solid Wall (After Brown et al. 2003)

2.2.1 Micro-Encapsulation Processes

The in-situ process is an extremely important component of this study, due to the fact that this was the process selected for the preparation of the microcapsules. An essential part of the microcapsule is the core shell itself (Massoth et al. 1965). The method utilized to generate the microcapsules core can be by liquid or gaseous phase, liquid or slurry, multiple wall capsule, etc. Within the in-situ process, an emulsification process produces a spherical core solid wall, as shown in Figures 2.2 and 2.3 (Brown et al. 2003).

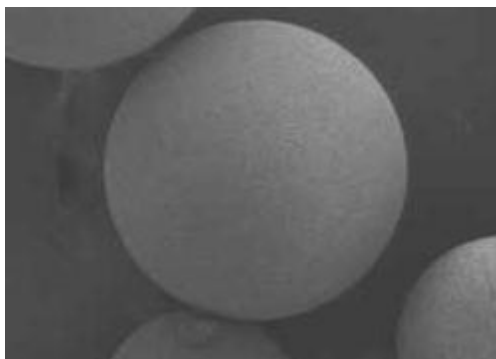


Figure 2.2 Microcapsule Solid Wall (After Brown et al. 2003)

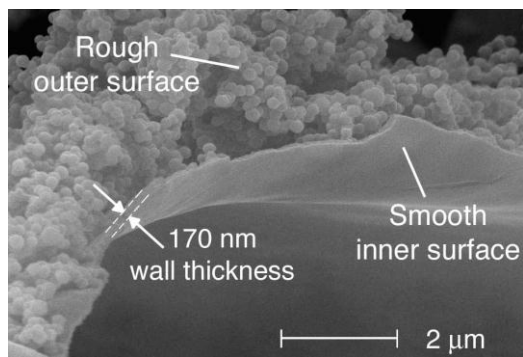


Figure 2.3 Representation of Wall Thickness (After Brown et al. 2003)

The second integral section of the microcapsule is the shell wall itself. In order to establish proper wall application, the type of materials for the given product desired must be selected. The material utilized must be appropriate to assist the microcapsules in enduring its required environment (Flinn and Nack 1967, a,b). In the case of the application of self-healing concrete, the wall must be rigid and strong enough to endure an aqueous condition as well as the concrete environment.

The deposited wall usually follows the outline of the generated core. This means that the final form of the shell wall for the capsule generated will be strongly affected by the core itself. This is why the selection of the materials, as well as the microcapsule process employed, will assist in distributing the core particles to achieve a smooth morphology (Massoth et al. 1965). The overall selection for the microcapsule process depends on multiple factors. These factors are the solubility of the core, the reactivity of the core to other chemicals and properties, and which method of core release should be evaluated. There are also other factors, such as storage release and reaction, and product performance (Massoth et al. 1965).

The in-situ process includes a combination of aqueous and interfacial polymerization. For the aqueous phase, the core material must be immersible in water. The walls will form when the dissolved material creates a ‘phase out’ and ‘wrap’ around core particles to make a suitable change (Flinn 1967). In order for this to occur, the system of the aqueous solution must be changed by the following factors: reduction in temperature, addition of chemical precipitating agent, or pH alteration. The micro-encapsulation process is also successful by utilizing an interfacial polymerization technique. The formation of a polymer at the interface between two liquid (Water and DCDP Interface) phases is known as interfacial polymerization (Hermann Nack 1967).

2.2.2 Effect of Temperature

Temperature plays a significant role in the design and manufacturing of microcapsules at elevated temperature by speeding up response time and enhancing poly-condensation advantage (Alexandridou and Kiparissides 1994). The microencapsulated monomer must be in the liquid phase in order to flow through the damage site. The original design is ineffective at low

temperature because DCPD is very likely in the solid phase. Diffusion of solid phase DCPD into the crack is slow or unlikely to occur at all (Brown et al. 2002).

2.2.3 Effect of RPM and Droplet Size

The overall distributions of the size of the microcapsules play an essential role in establishing the surface area in which contents are unconfined. As the microcapsules originate from the solution, various sizes of spherical capsules will be developed. The stirring rate has the greatest effect on drop sizes (Ovez et al. 1997). In using the urea-formaldehyde method, drop size variation while polymerization is occurring, is a direct function of time. Drop sizes during this process also have a direct impact on the crosslink of urea and formaldehyde (Ovez et al. 1997).

The agitation rates, as well as the stirrer being utilized, are essential in establishing diameter control. As blade driver is not a shear stirrer, the microcapsules will not be uniform (Jyothi et al. 2010). If the agitation rate is fast, the microcapsules generated will be of a smaller diameter. As the agitation rate decrease, so does the overall size of the microcapsule (Alexandridou and Kiparissides 1994). This means that there is a direct relationship on a linear log-log scale between average diameter and agitation rate (Brown et al. 2003). As previously mentioned, the droplet size along with the shear agitation rate is critical in the successful developing of microcapsules.

2.3 CHARACTERIZATION OF MICROCAPSULES

Microcapsules can be evaluated and characterized using numerous techniques. These techniques include Transmission Electron Microscopy (TEM), Atomic Force Microscopy, Scanning Electron Microscope (SEM), etc. SEM was the method adopted in this study due to its ability to best meet the requirements for the analysis of microcapsules. The following sections present each characterization method as well as their analysis processes.

2.3.1 Transmission Electron Microscopy Analysis

Both SEM and TEM are adequate methods for the characterization of microcapsules or nanocapsules. Specific size elements and nanoparticles are not visible because they are smaller than visible wavelengths, therefore to see nanoparticles, smaller wavelengths are required. As one gets closer to the object the depth of focus broadens, the aperture is larger, but the focus is worse, which leads to the limit of resolution (the ability to distinguish something into its separate

components) (Williams 1996). As a result, the concept of scanning electron techniques is simple; the wavelength of smaller dimensions correlates to smaller dimensions observable.

In the 1930's, transmission electron microscopy (TEM) was first built followed by the scanning electron microscopy (SEM). Scanning electron microscopy is used for 2-D surface imaging with resolution near 1 nm. Used with energy dispersive spectroscopy the elemental composition can be derived. Using a similar technique, TEM can collect the transmitted electrons. This can be instrumental in analyzing extremely small micro-capsules or nano-capsules. Higher resolution near 0.2 nm can be achieved; however, the sample must be a thin film to allow for electron transmittance (Hornyak et al. 2008).

TEM accelerates electrons that either pass through or deflect the subject material. Elastic scattering is when there is no energy loss whereas inelastic scattering is due to heterogeneities such as density changes, boundaries, and defect. The information on electrons deflected and passing through is gathered to produce a high magnified resolution. Higher voltages are required for thicker samples or better lateral resolution. As a result, TEM is limited to thin films (Hornyak et al. 2008). Although TEM is an acceptable method for characterization, this system was not utilized due to the fact that the microcapsules were no smaller than 10 μm in length.

2.3.2 Atomic Probe Microscopy

The scanning probe techniques are the true techniques for determining 3D Micrometer measurements. This method can be utilized for micro-capsule characterization in specifying definite and precise measurements. These methods are not dependent on the wavelength like optical and electron microscopy. Instead, it is based on the principle of electron tunneling. Two common techniques are scanning tunneling microscopy (STM) and atomic force microscopy (AFM). STM allows for 3-D surface imaging including the height dimensions at resolution near 0.1 nm. Using a tunneling current applied to a probe tip that is rastered across the surface, the electrons from the tip jump to the surface at a measurable current proportional to the distance from the surface. The problem is that the material imaged must be conducting. To address this barrier, the AFM measures the force between the probe and the surface, thus, eliminating the need of a conductive material. The probe can be made of several materials such as silicon and tungsten but the main importance is the sharpness of the point relating to the image clarity (Hornyak et al. 2008).

Recent developments in microencapsulation characterization of cementitious materials have begun to show the importance of AFM in determination of mechanical properties. Various experiments have used AFM with nanoindentation probe to study the local mechanical properties coupled with high-resolution imaging. The qualitative results are proportional to the modulus of elasticity. To quantify the modulus of elasticity, nanoindentation tests must be used. Studies have used statistical analysis to relate several elastic moduli from various phases to relate to the qualitative results obtained from the AFM to estimate the elastic moduli profile (Mondal et al. 2005).

2.3.3 SEM Analysis

Figure 2.4 is an illustration of an operational SEM machine located at Louisiana State University. The S-3600N Hitachi ESEM Microscope has ability to generate extraordinary digital images of the surface of a sample. This system consists of large sample chambers, which can analyze samples up to 254 mm in diameter, 70mm in height and 2kg in weight. The system utilizes a pressurized adjustable mode that enables the analysis of non-conductive samples, which eliminate the need for special sample preparation of the non-conductive samples (Danilatos 1990). The SEM also encompasses a specimen chamber with 12 ports, which ensures the best geometry for the multiple detectors and accessories. This pressure scanning electron microscope has a resolution of 3 nm at 25 kV under high vacuum conditions and 4.5 nm at 25 kV under variable pressure conditions. Variable Pressure technology permits examination of virtually any type of sample without the need for traditional sample preparation techniques (Danilatos 1990).



Figure 2.4 Hitachi S-3600N ESEM Microscope

The SEM tool consists of seven primary components:

1. Beam Generation – This system is located at the top of the microscope and generates the primary electron beam.
2. Beam Interaction – This includes the interaction and involvement of the sample with the electron beams, and the multiple signals that can be detected.
3. Vacuum System – The vacuum system eliminates the dispersion and scattering of electrons due to the interaction of the electron beam forcing collisions with different molecules within the chamber.
4. Beam Manipulation– This system controls the size, shape and position of the beam on the samples surface. It encompasses electromagnetic lenses and coils, which are located at the microscopes column.
5. Signal Processing – This includes an electronic system, which handles the manipulation of the initial image, and processes the generated image by the detection system.
6. Detection System – This system consists of multiple detectors, each of which is sensitive to the multiple energy particles that occur on the specimens' surface.
7. Display and Record System – This incorporates a cathode ray tube which allows recording of the analysis utilizing a photographic or magnetic media, and enables visualization of an electronic signal.

These subsystems work together in determining specifics of a micrograph such as: resolution, depth of field, contrast magnification and brightness. When dealing with the analysis portion of the SEM, the following occurs in the analysis process. When an electron beam hits a specimen, part of the beam will become scattered by other particles and the rays emitted tend to be very characteristic of the element from which they originated (Goldstein 2003). This electron beam – sample interaction will eventually cause the ray energy to dissipate, as well as change the wavelength from when it was originally emitted. The possibility of identifying a ray after it

loses some its energy, is extremely common at the low energy spectrum, and in retro-respect will decrease towards the high energy end. This is known as uncharacteristic rays. They are called this term due to the energy and wavelength they possess and because they do not have the original character traits from which they originated from (Egerton 2005).

Characteristic x-rays have the ability to interfere with primary identification once elements are in low concentrations. They are represented by low energy characteristic x-ray lines, where the background is significantly higher. This is why the WDS (Wavelength Dispersive Spectroscopy) detector is set to detect a specific range of wavelengths. Wavelengths which are not in this range cannot be detected (Goldstein 2003). The WDS detector is usually preset for a small range of wavelengths and the sensitivity of the detector is greater which allows for greater accuracy in analytical work.

Using this type of detector, however, is cumbersome when dealing with an unknown specimen because of the many spectra that need to be gathered to determine the elemental composition of an unknown sample. With any type of SEM studies, it is important that the sample be as smooth as possible (Goldstein 2003). Topography will influence the X-ray counts and gives a poor determination of the elemental composition. This is the main reason X-ray analyses are often difficult to use with biological samples.

2.3.4 SEM Procedures and Imagery Analysis

The following sections provide a detailed explanation of sample preparation as well as procedures and techniques that are normally utilized for analysis of a specimen.

SEM Sample Preparation

Microcapsule preparation for SEM is generally prepared by a technique called ‘sputtering’. This process involves a large amount of heavy particles being sprayed on a specimen under a gaseous glow discharge between an anode and cathode, which will cause the erosion of the prepared specimen (Goldstein 2003). By sputtering a specimen, the following benefits are involved:

- Increase in thermal conduction;
- Improved secondary electron emission;
- Reduced beam penetration with improved edge resolution;
- Protection of specimens which are beam sensitive;
- Reduction in microscope beam damage.

Under glow condition discharge, ion bombardment of the cathode occurs, which will result in the erosion of the cathode material (Plasma Sputtering). This will result in the omni-directional deposition of the sputtered atoms, which form coatings of the original cathode material on the surface of the sample and work chamber (Reimer 1998). This is an important method to use for SEM samples that require an electrically conductive thin film for the sample. The process utilized for the Microcapsules is called D.C. (Direct Current) coater. This method utilizes a negative cathode on the specimen to be sputtered, and to locate samples that are to be coated on the anode (Reimer 1998). A typical system utilized during platinum sputtering of the microcapsules, consisted of a two stage rotary vacuum pump and an inert gas; which was admitted to a chamber by a controlled valve. This process allowed defined characteristics and clearer images for the SEM analysis.

When evaluating a specimen, a sample must possess the following characteristics:

1. Adequate Dimension
2. Stable Stage for the Vacuum System
3. Electrical Conductivity
4. Retain Natural State Characteristics

When metallic specimens are utilized, many of them require very little manipulation or preparation. If it was required to use a specimen such as a unique mineral, clay or elastic, it would need to be coated with a conductive metal. If biology samples are utilized, such as flower petals and insects, the natural water retention will give them sufficient conductivity to be evaluated. Although this can be utilized, it is not recommended due to the fact that it will contaminate the microscope (Reimer 1998). The procedure adopted in analyzing platinum coated microcapsules was as follows:

1. A sample was adequately prepared (coated using sputter technique), placed in the specimen holder and measured by the measuring device (see Figure 2.5)
2. The SEM chamber door was then opened, and the sample was then carefully placed inside the sample holder, and secured (See Figure 2.6).
3. The door was then closed, and the “EVAC” button was pressed simultaneously.
4. The user must then wait until the “Vacuum” says ready and the status bar turns blue.

5. The student is then able to select “Go Home” and change the Specimens Size & Height. In this study, it was 55 mm.
6. Next, the Z/Tilt is changed from 5 – 15 mm. This allows us to examine the specimen much closer (acceptable range is 5.0 – 25).



Figure 2.5 Loading of the Sample in the Chamber

5. After the user has input all the specifications and requirements that needed to be changed, the user shall select HV at the top right corner of the monitor and ensure system is in ABC mode. * Do not select ASF *
6. Utilizing proper technique and procedures, the user then adjusts “Stigmator/Alignment” X & Y to ensure beam alignment to improve image quality.
7. Once complete, the user is able to use the proper procedures using the Magnification, Contrast, Brightness and Focus in order to attain the desired image quality for analysis.
8. Once the user selects the image the user desires to utilize for analysis, the User must select “H.R.” Capture. This allows the system to collect the best image possible (See Figure 2.7)

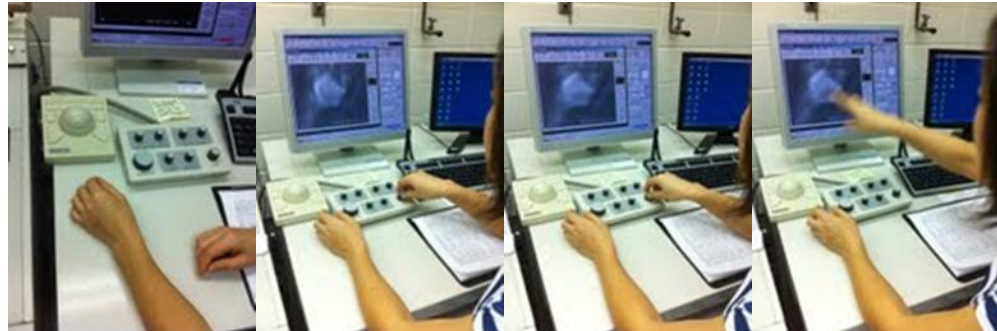


Figure 2.6 User Operation of the Hitachi S-N3600

9. The user must then manually select the image on the left hand side, left click on the image and select “PCI”. This allows the transfer and saving of an image on another program.
10. Once the image has been saved, close the window and select “TV”. Complete steps 7 through 11 until the user had gathered all of the imagery that he deems sufficient (see Figure 2.7).



Figure 2.7 User Adjusts parameters to generate a series of Quality Images

11. When ready for shutdown, ensure all pictures are deleted and select “HV”.
12. After one minute, press “EVAC” on microscope bottom department.

13. After all Vacuum pressure is released, carefully open chamber door and remove specimen.
14. Close door gently and contact lab technician to inform that you are complete with the use of the equipment.

In retrospect to the SEM, the following are required to effectively construct an electron beam:

- High voltage
- Filament Current
- Bias Controls

Specific components such as the beams gun, specific lenses and apertures must be properly aligned in order for the beam to be centered on the sample. Also, proper beam alignment, which is implemented by small adjustments to the petite deflection coils, is a necessity as well. A thorough understanding was developed in comprehending the restriction of the SEMs restrictive aperture (Reimer 1998). By understanding the difference between large (allow additional electrons through thereby better recording of micrographs under low noise conditions) and small (allow for a much better beam resolution) apertures, one is able to manipulate the SEM in order to develop a better overall images.

The overall goal in the utilization of SEM is to acquire the best resolution possible. In doing so, the user must inquire and determine the instrument's best resolution and not the capability of its magnification (a normal microscope utilizes lens magnification whereas SEM relies on its beam and emitting of electrons). Understanding theories such as Empty Magnification, Depth of Field, Polymerization of the beam is essential in the evaluation of a sample. An additional goal in attaining exceptional resolution is knowing and understanding that the signal level for detection will be decreased due to the minute spot impacting the specimen.

The emission of the specimen and its topography efficiency play a huge role on the signal level as well. Because some specimens are capable of producing more secondary electrons, this will result in a higher atomic numbers, which in turn will promote better emission efficiency. If

a specimen surface is rough, it will provide more surface area, therefore emitting a better signal from the specimen.

One of the major user controlled factors that contribute to brightness is the electrons emitting from the specimen. There are also other factors that contribute to this such as Brightness control knob, recording film speed, etc. In having a thorough understanding of SEM, will enable a user to develop a detailed high resolution image for evaluation and analysis.

2.4 REFERENCES

Alexandridou, S and C. Kiparissides. Production of oil-containing polyterephthalamide microcapsules by interfacial polymerization—an experimental investigation of the effects of process variables on the microcapsule size distribution. *Journal of Microencapsulation*, Vol. 11, 1994, pp. 603–614.

Brown, E. N., M. R. Kessler, N. R. Sottos and S. R. White. In situ poly(urea-formaldehyde) microencapsulation of dicyclopentadiene. *Journal of Microencapsulation*, Vol. 20, No. 6, 2003, pp. 719–730.

Brown, E. N., N.R. Sottos, and S.R. White. Fracture testing of a self-healing polymer composite. *Experimental Mechanics*, Vol. 42, 2002, pp. 372–379.

Danilatos, G.D. Foundations of Environmental Scanning Electron Microscopy. *Advances in Electronics and Electron Physics*. Vol. 71, 1988, pp. 110-248.

Danilatos, G.D. Design and construction of an environmental SEM (part 4). *Scanning*, Vol.12, 1990, pp. 23–27.

Dry, C. and N. Sottos. Smart Structures and Materials 1993: Smart Materials. *SPIE Proceedings*, Vol. 1916, Feb 1–4, 1993, Albuquerque, NM. Varadan, VK, Ed., SPIE: Bellingham, WA, 1993

Dry, C. Procedures developed for self-repair of polymeric matrix composite materials. *Composite Structures*, Vol. 35, 1996, Vol. 263-269.

Dunker, A. K., E.J. William, R. Rammon, B. Farmer, and S. J. Johns. Slightly bizarre protein chemistry: urea-formaldehyde resin from a biochemical perspective. *Journal of Adhesion*, Vol. 19, 1986, pp. 153–176.

Egerton, R. F. (2005) *Physical principles of electron microscopy : an introduction to TEM, SEM, and AEM*. Springer, New York, NY, 2005

Flinn^a, J. E., and Nack, H., Advances in microencapsulation techniques, *Battelle Technical Review*, Vol. 16, 1967, pp. 2-8.

Flinn^b, J. E., and Nack, H., What is happening in microencapsulation. *Chemical Engineering*, Vol. 74, 1967, pp. 171-178.

FHWA-RD-01-156, Corrosion cost and preventive strategies in the United States. September 2001, CC Technologies Laboratories, Inc. to Federal Highway Administration (FHWA), Office of Infrastructure and Development

Goldstein, J. *Scanning electron microscopy and x-ray microanalysis*. Kluwer Adademic/Plenum Publishers, 2003

Hornyak, G.L., J. Dutta, H.F. Tibbals, and A.K. Rao. *Introduction to Nanoscience*, CRC Press, Florida, 2008.

Jyothi, N.V.N., P.M. Prasanna, S.N. Sakarkar, K.S. Prabha, P.S. Ramaiah, and G.Y. Srawan. Microencapsulation Techniques, Factors Influencing Encapsulation Efficiency. *Journal of Microencapsulation*, Vol. 27, 2010, 187-197.

Lee, L. H. *Adhesive Bonding*. Plenum, New York, 1991, pp. 239-291.

Massoth, F. E., W. E. Hensel Jr. and W.W. Harlowe Jr. Basic studies of the Encapsulation process. Industrial and Engineering Chemistry Process Design and Development, Vol. 4, 1965, pp. 6-13.

Mondal, P., S.P. Shah, and L.D. Marks. "Nanoscale characterization of cementitious materials." *ACI Materials Journal*, Vol. 105, Ed. 2, 2005, pp. 174-179.

Ovez, B., B. Citak, D. Oztemel, A. Balbas, S. Peker and S. Cakir. Variation of droplet sizes during the formation of microspheres from emulsions. *Journal of Microencapsulation* Vol. 14, 1997, pp. 489-499.

Rammon, R. M., W.E Johns, J. Magnuson, and A.K. Dunker. The chemical structure of UF resins. *Journal of Adhesion*, Vol. 19, 1986, pp. 115–135.

Reimer, L. *Scanning electron microscopy : physics of image formation and microanalysis*. Springer, 1998

Schlangen, E. 2005, Self-healing phenomena in cement-based materials.

White, S. R., N.R. Sottos, P.H. Geubelle, J.S. Moore, M.R. Kessler, S. R. Sriram, E. N. Brown, and S. Viswanathan. Autonomic healing of polymer composites. *Nature*, Vol. 409, 2001, pp. 794–797.

Wool, R. P. Ch. 12 *Polymer Interfaces: Structure and Strength*, Hanser Gardner, Cincinnati, 1995, pp. 445-479.

Zihlif, A.M., Z. Elimat, and G. Ragosta. Thermal and mechanical characterization of polymer composites filled with dispersed zeolite and oil shale. *Journal of Composite Materials*, Vol. 45, Is. 11, 2011, pp. 1209-1216.

CHAPTER 3

MICRO-ENCAPSULATION OF SELF-HEALING CONCRETE PROPERTIES

3.1 INTRODUCTION

Concrete is one of the most used building materials in the world. Concrete has a large load bearing capacity for compressive load, but the material is weak in tension. That is why steel reinforcement bars are embedded in the material. The steel bars carry the load when the concrete is loaded in tension. The concrete on the other hand protects the steel bars from the environment and prevents corrosion from taking place. However, cracking in the concrete presents a problem. The ingress of water and ions take place and deterioration of the structure starts with the corrosion of the steel. To increase the durability of the structure either the cracks that have formed are repaired or in the design phase, extra reinforcement is placed in the structure to ensure that the crack widths stay within a certain limit. Durability is one reason to prevent cracks or limit crack widths. Other reasons are water tightness of structures, loss of stiffness and aesthetic reasons. This extra reinforcement is then only needed for durability reasons (to keep the crack widths small) and not for structural capacity. With current steel prices, this extra steel is not desirable.

With concrete bridges, corrosion is the number one cause of deterioration for the concrete infrastructure throughout the nation. The dollar impact of corrosion on reinforced-concrete, pre-stressed concrete and steel bridges is considerable but the indirect costs (those incurred by users) increase expenses tenfold (FHWA 2008). For example, a traffic tie-up or detour caused by a bridge failure or its rehabilitation and maintenance can result in wear and tear on automobiles, increased gasoline use, delays in product transport, missed appointments, and other inconveniences that result in lost dollars. A typical dilemma for bridge management is how to allocate limited funds for construction, rehabilitation, and maintenance. Funding typically comes from city, state, and federal sources that often have spending restrictions. It is, therefore, difficult to make optimal decisions about when and how to inspect, repair, or replace bridges while minimizing the impact on drivers (FHWA). Supporting the use of a more durable, self-healing concrete, will further reduce the large direct and indirect expenses associated with bridge corrosion. By incorporating self-healing concrete properties within concrete mixes, the process

will not only change concrete quality design and control methods, but the goal is to positively impact the overall construction process as a whole.

The need for self-healing concrete is further supported by the latest ASCE report. More than 26% of the nation's bridges are either structurally deficient or functionally obsolete. While some progress has been made in recent years to reduce the number of deficient and obsolete bridges in rural areas, the number in urban areas is rising. A \$17 billion annual investment is needed to substantially improve current bridge conditions. Currently, only \$10.5 billion is spent annually on the construction and maintenance of bridges.

Before self-healing microcapsules can be applied effectively to concrete matrixes, specific preparation parameters must be understood to control microcapsule properties. Therefore, the objective of this study is to evaluate the effect of pH, temperature, and agitation rate during the microencapsulation process on the resulting microcapsule morphology.

3.2 BACKGROUND

3.2.1 Overview of Self-Healing Methods

There are numerous applications and methods used in self-healing concrete. An application of self-healing that has been implemented is known as Hollow Glass Reinforced Polymer. FRP's (Fiber-Reinforced Polymer's) have great performance characteristics in relation to strength and stiffness. FRP's allow for a versatility and flexibility in performance. It has been proven that FRPs not only give an advantage to incorporate a healing agent, but they also have positive structural improvements (Kessler 2002). When failure, overstressing or broken fibers occur, the healing agents flow into the damaged area, repairing the damaged structure.

Glass fibers, which contain specific healing agents, are categorized in two main types. One type can serve as a one-part adhesive, such as cyanoacrylate (Kessler 2002). The system can also serve as a two-part epoxy system, containing both a resin and a hardener. Both of these methods are located perpendicular to one another; however, one is implemented within the matrix itself and one within the fibers (Kessler 2002). It has been shown from previous studies that these hollow fibers are multifunctional; since the fibers themselves store a liquid healing agent while simultaneously provide structural reinforcement.

By utilizing this method of self-healing, one can generate a self-healing concrete material having the same mechanical characteristics as normal concrete. The process that was used in this study was that of micro-encapsulation of self-healing concrete properties, specifically DCDP and sodium silicate. The purpose of the microcapsule shell is to provide a protective barrier between the catalyst and DCPD to prevent polymerization during the preparation of the composite.

The two self-healing methods were DCDP and sodium silicate. Dicyclopentadiene ($C_{10}H_{12}$) is a white crystalline solid/Clear Liquid solution (depending on its potency) with an energy density of approximately 10,975 Wh/l. Its main use within industry and private practice is for resins/unsaturated polyester resins (Xiaofang 2005). This chemical can be used as a monomer in polymerization reactions, such as: ring-opening metathesis polymerization or olefin polymerization. Sodium Silicate (Na_2O_3Si), which is also known as liquid glass, is a sodium metasilicate compound. This solid or aqueous solution can be used in cements, automobiles and even textile and lumber processing. In concrete applications, this product is used to reduce the concrete porosity. When added, a chemical reaction occurs with the excess of $Ca(OH)_2$, which is already present in concrete (Greenwood 1997). When (Na_2O_3Si) reacts with $Ca(OH)_2$, the concrete permanently binds with the silicates at the surface. This makes the product a great sealer as well as a great water repellent.

The microcapsule self-healing method was selected, due to self-healing chemicals' ability to independently resolve issues such as internal cracking and micro-cracking. When the cracks occur, they initiate imminent path towards structural failure. By filling these voids and cracks with self-healing materials, these structures will have a longer life cycle along with a less likelihood of destruction from unwanted moisture and corrosion wear (Brown 2003). Although DCDP is an exceptional healing agent alone, in order for the agent to achieve maximum effectiveness, an appropriate interaction is required to polymerize the healing agent within the damaged area. A process called ring opening metathesis polymerization (ROMP) provides the following advantage for the self-healing microcapsules (White et al. 2001):

1. A more durable long lasting shelf life;
2. A low monomer viscosity and volatility;

3. Increased rapid polymerization during ambient conditions; and
4. Low shrinkage rate during polymerization.

The ROMP process utilizes a Grubbs Catalyst (transition metal catalyst), which incorporates a high metathesis method. The use of this catalyst allows multiple chemical groups to be utilized within the chemical process (such as oxygen and water). When DCDP encounters this Grubbs Catalyst, polymerization occurs (Brown 2005). Sodium silicate, however, does not require a matrix and can be used as an individual healing component. The first reaction (R1) consists of sodium silicate reacting with calcium hydroxide, which is a product of cement hydration (Nonat 2004). The second reaction (R2) occurs between sodium hydroxide and silica. R1 produces a calcium-silica-hydrate gel, known as (C-S-H). This method creates a binding material normal to concrete matrix. What is essential in both processes is the mending agent that resides in an aqueous environment within the microcapsule itself (Nonat 2004). Water enables the hydration of the damaged cement and also allows, further bonding of the mending agent. The C-S-H and N-S-H gel will fill the crack, and subsequently permits recovery of strength. It is important to note that C-S-H and N-S-H complex process will occur rapidly and then much slower, respectively. Both processes support the presence of the aqueous mending agent, which again provides further integrity of the concrete by creating a bond, healing the crack (Nonat 2004).

3.2.2 Microencapsulation Procedures

There were over 100 trials attempted that involved the stabilization for the two different microencapsulation methods that were utilized for DCDP, as well as sodium silicate. The first microencapsulation procedure that was attempted was that of the Autonomic. This was one of the first attempts to the microencapsulation procedure utilizing the Urea-Formaldehyde method. This method focused on developing a procedure that would control the properties of the microcapsule geometry, and its mechanical triggering system (Tseng 2005). When evaluating the wall thickness parameters, it was understood that microcapsule walls that were too thin would fail during the manufacturing process. In retrospect, capsule shells that are too thick will not allow wanted breaking or fracturing of the shell as the crack penetrates through the microcapsules plane. This method also achieved a specific robustness, virtual toughness, and a strong interface with the matrix and the microcapsule itself (Tseng 2005). This focus of interest provided a basic orientation and baseline to begin further studies and trials.

A more defined and developed process of micro-encapsulation using the urea-formaldehyde method was developed by Brown et al. (2003). The in-situ encapsulation method for water-immiscible liquids, by the reaction of urea with formaldehyde at acid pH, which was outlined by Dietrich et al., was the foundation of this extensive method. S.R. White and his team were able to streamline the micro encapsulation of DCDP by controlling its diameter as well as the morphology.

Although the shell wall thickness was analyzed and thoroughly explained, there is a minimum amount of literature, which incorporated information to specifically control its parameters. For example, it was annotated that too much ammonium chloride or resorcinol, reduced quantities of DCPD, tainted beakers, an unbalanced or unaligned mixer and lower initial pH will increase the thickness of the microcapsules shell wall. With certain standards and practices in place, all of these factors can be controlled. However, if there was a desire to change the thickness of the capsule wall, the pH would be the likely candidate for evaluation.

Micro-encapsulation of sodium silicate has -been successfully accomplished by using the polyurethane micro-encapsulation procedures only. This process, also using in situ synthesis, is an interfacial polymerization, which was adapted from (Jinglei Yang et al 2008). The following chemicals were utilized during this process: Span 85, polyethyleneglycol (PEG), toluene, methylene diisocyanate (Basonat), dibutyl tin dilaureate, etc. Although theoretically possible, micro-encapsulation of the Sodium Silicate using the Urea-Formaldehyde method has never been successfully accomplished before.

3.3 EXPERIMENTAL PROGRAM

3.3.1 Materials

The chemicals utilized in the preparation of the microcapsules based on in-situ polymerization are presented in Table 3.1.

Table 3.1 Required Chemicals for Interfacial Polymerization Synthesis

Chemical	Function	Manufacturer
Urea	Creates endothermic reaction in water	The Science Company
Ammonium Chloride	Assists with curing Process	The Science Company
Resorcinol (Technical Grade Flake)	Reacts with formaldehyde and is a chemical intermediate for the synthesis process	NDSPEC Chemical Corporation

Table 3.1 Continued		
Chemical	Function	Manufacturer
ZeMac E60 Copolymer	Improves mechanical properties	Vertellus Specialties, Inc.
ZeMac E400 Copolymer	Improves mechanical properties	Vertellus Specialties, Inc.
Octanol	Prevents surface bubbles	Oltchim
Hydrochloric Acid	Lowers pH	The Science Company
Sodium Silicate	Reacts with Ca(OH) ₂	The Science Company
Sodium Hydroxide	Increases pH	The Science Company
Formaldehyde	Reacts with urea during synthesis process	The Science Company
Grubbs Catalyst	Reacts with DCDP and polymerizes	Materia, Inc.
DETA (diethylenetriamine) Mix with EPON 828	Used in synthesis of catalysts, epoxy curing agent, and corrosion inhibitors	Huntsmann
DCDP	Selected Resin to Heal Concrete Crack	Texmark- 87% & 89% Purity Cymetech- 99% Purity

3.3.2 Equipment

The Mettler Toledo Scale and Symmetry Cole Palmer Scale were utilized to measure all the solid and liquid chemicals utilized throughout the procedures and trials. To dissolve the co-polymer in water, a 120V Hotplate Stirrer VWR and 2510 Branson Sonicating Water Bath were used. All the water used for the synthesis of the microcapsule is DI (deionized water) water provided from the BarnStead Water Pure Nano Filtration system. Once all the chemicals were added and an emulsion was created, the mixture was continuously stirred and heated by the SuperNova Thermo scientific hotplate. However, for the in situ interfacial polymerization process, the IKR RW 20 Digital Stirrer with the 55 mm three bladed shear stirrer was used to allow for better standardization and efficiency due to the much stronger shear three-blade stirrer. Once the microcapsules were synthesized, they were vacuum filtered using a Cole Palmer Air Admiral Vacuum Filtration System with 0.22 µm Nonpyrogenic Sterile Polystyrene Filters.

3.3.3 DCDP Micro-Encapsulation Procedures

In Situ Procedure

This procedure was accomplished by using an in situ polymerization procedure, in an oil-in-water emulsion. First, 200 ml of DI water was placed in a 1000 ml beaker. Next, 50 ml of 2.5 wt% EMA copolymer was dissolved using a magnetic stirrer and ultra sound water bathe; and an aqueous solution was developed. Agitation was implemented by using an IKA RW 20 digital mixer, with a driving 55 mm low shear three-bladed mixing propeller (Cole Parmer) placed just above the bottom of the beaker. Under agitation, 5.00 g urea, 0.50 g resorcinol and 0.50 g ammonium chloride was then dissolved in the solution. The pH was set to 3.7 by using sodium

hydroxide (NaOH) and hydrochloric acid (HCl) drop-wise with a disposable pipet. The high agitation rate of 800 rpm developed surface bubbles; therefore two to three drops of 1-octanol were added to eliminate this issue. The solution was allowed to stabilize for approximately 6 – 8 minutes at the appropriate pH and rpm agitation rate, before 100 ml of DCPD at a slow stream rate. The solution was allowed to stabilize for 13 – 15 minutes before 12.67 g of 37 wt% aqueous solution of formaldehyde was finally added to the emulsion. The solution was then wrapped and covered with aluminum foil, and slowly heated to a temperature of 55° C. After 4 hours of continuous agitation the mixer and hot plate were switched off. Once cooled to ambient temperature, the suspension of microcapsules was separated under vacuum filtration. The microcapsules were rinsed with DI water three times with 500 ml. of DI water, and then allowed to air dry for 48 - 72 h. The procedure has been outlined in Figure 3.3. Figure 3.4 is a representation of the materials, equipment and microcapsule filtration.

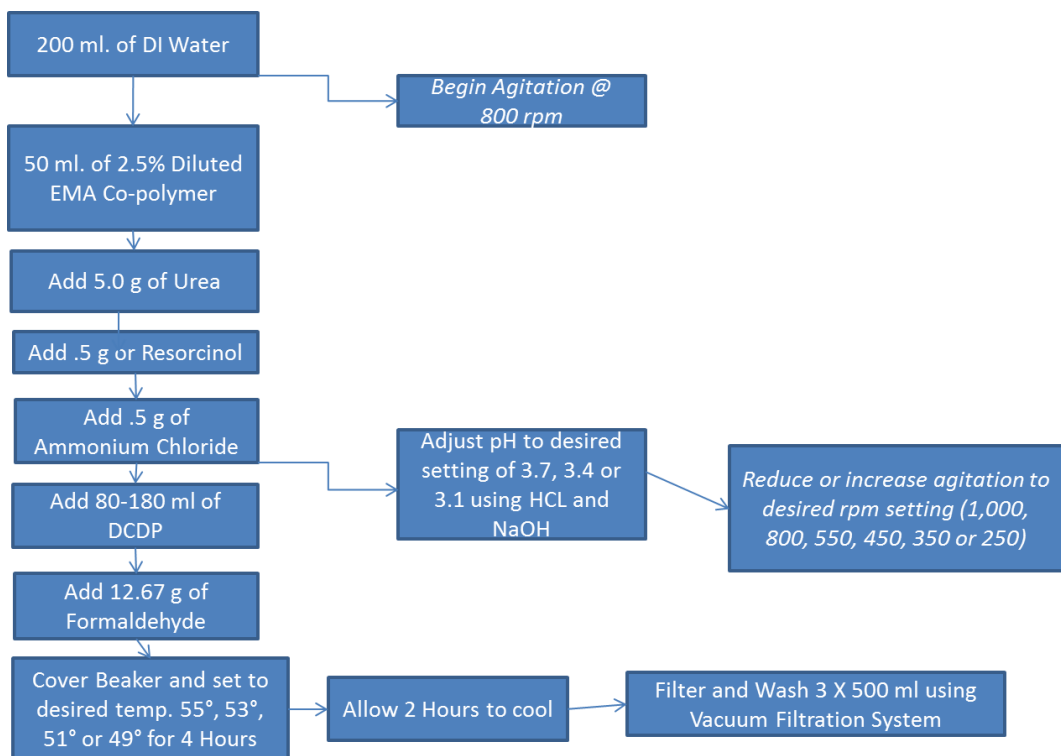


Figure 3.3 DCDP In Situ Process

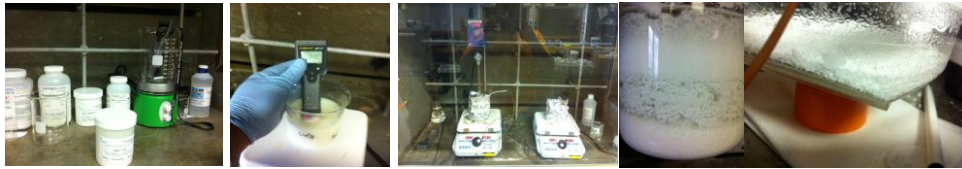


Figure 3.4 Microencapsulation Synthesis Process

3.3.4 Sodium Silicate Microencapsulation

In Situ

This procedure was accomplished by using an *in situ* polymerization procedure, in an oil-in-water emulsion. First, 200 ml of DI water was placed in a 1000 ml beaker. Next, 100 ml of 5.0 wt% EMA copolymer was dissolved using a magnetic stirrer and ultra sound water bathe; and an aqueous solution was developed. Agitation was implemented by using an IKA RW 20 digital mixer, with a driving 55 mm low shear three-bladed mixing propeller (Cole Parmer) placed just above the bottom of the beaker. Under agitation, 7.00 g urea, 0.50 g ammonium chloride and 0.50 g resorcinol were then dissolved in the solution. The pH was set to approximately 3.0 by using sodium hydroxide (NaOH) and hydrochloric acid (HCl) drop-wise with a disposable pipet. The high agitation rate of 800 rpm developed surface bubbles; therefore two to three drops of 1-octanol were added to eliminate this issue. The solution was allowed to stabilize for approximately 6 – 8 mins. Next, 171 ml. of DI water was added to 60 ml. of an aqueous sodium silicate. The solution was allowed to agitate for approximately 5 min. While under agitation, HCL was slowly added to the solution to form a gel/aqueous solution. 100 ml. of the gel/aqueous solution was then slowly added to the emulsion while maintaining a pH of 3.0 – 3.5. While still under agitation, the pH was adjusted to achieve a goal of 3.3. The solution was allowed to stabilize for 13 – 15 minutes before 18.91 g of 37 wt% aqueous solution of formaldehyde was finally added to the emulsion. The solution was then wrapped and covered with aluminum foil, and slowly heated to a temperature of 55° C. After 4 hours of continuous agitation the mixer and hot plate were switched off. Once cooled to ambient temperature, the suspension of microcapsules was separated under vacuum filtration. The microcapsules were rinsed with DI water three times with 500 ml. of DI water, and then allowed to air dry for 48 - 72 h. The procedure has been outlined in Figure 3.4.

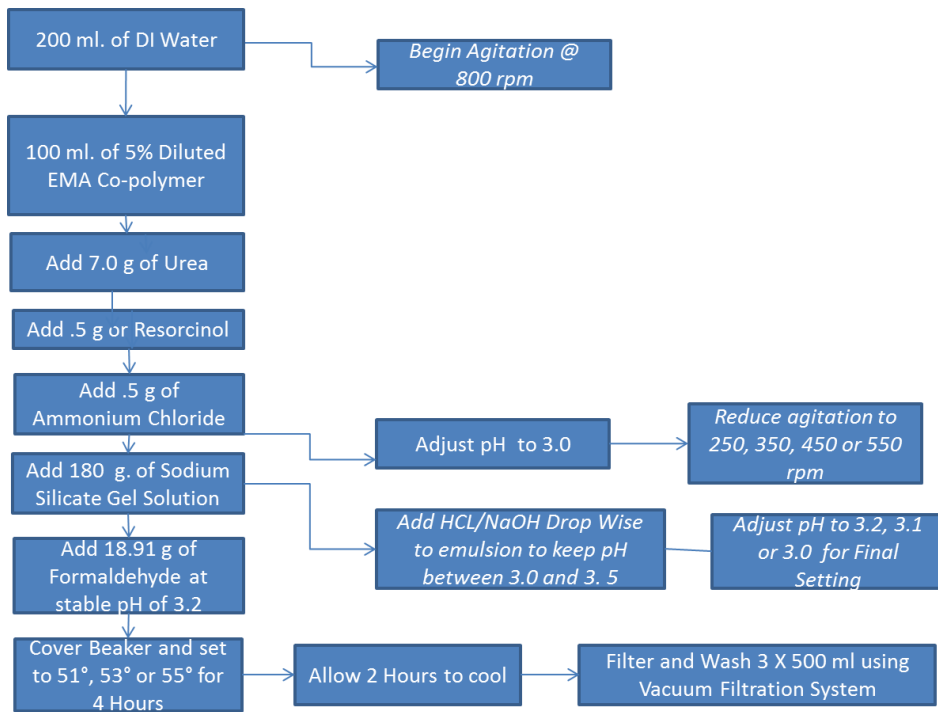


Figure 3.4 Sodium Silicate In Situ Process

Test Factorial

An experimental program was developed to evaluate the effects of preparation parameters, namely, temperature, agitation rate, and pH on the shell thickness and size (diameter) of the microcapsules. Table 1 presents the experimental factorial followed in this study. Two healing agents were evaluated, DCDP and sodium silicate. During synthesis, the agitation rate, temperature, and pH were varied. The agitation rate was varied at 6 levels for the DCDP synthesis and at 4 levels for the sodium silicate synthesis; while the temperature and pH were kept constant. Similarly, to test the effect of the temperature, three levels were used while the pH and agitation rate were kept constant. Three pH levels were used while the temperature and agitation rate were kept constant. This resulted in a total of 10 synthesis methods tested using DCDP and 8 synthesis methods tested using sodium silicate. All levels are reflected in Experimental Factorial Table 3.1.

Table 3.1 Experimental Factorial

Variable	Content	Number of Levels
Healing Agent	DCDP and sodium silicate	2

Table 3.1 Continues on Next Page

Table 3.1 Continued

Variable	Content	Number of Levels
DCDP Agitation Rate (rpm)	250, 350, 450, 550, 800, and 1000	6
Sodium Silicate Agitation Rate (rpm)	250, 350, 450 & 550	4
DCDP Temperature (°C)	49, 52, and 55	3
Sodium Silicate Temperature (°C)	51, 53, and 55	3
DCDP pH value	3.1, 3.4, and 3.7	3
Sodium Silicate pH Value	3.0, 3.1, and 3.2	3

3.4 RESULTS AND ANALYSIS

3.4.1 Microcapsule Parameter Analysis

After extensive literature review, it was determined that numerous factors can affect morphology and shell thickness. It was determined through analysis, that the pH has the largest effect on the thickness of the shell. The outer surface of the microcapsule has a rough permeable layer, whereas the inside is smooth and free of cavities. Factors that can affect the morphology are unclean components or glassware, not enough DCDP/Sodium Silicate to allow encapsulation, or too much ammonium chloride or resorcinol. Other factors can include improper utilization of equipment, such as wrong size stirrer or driver size, pH meter not being calibrated correctly, and poor monitoring methods of temperature and agitation rate. The controlling parameters to stabilize and sustain microcapsules are discussed in the next sections. The microcapsule synthesis yield results are represented below. The highest yield for DCDP was 79.02 @ RPM: 350, TEMP: 55, pH: 3.7. The highest yield of Sodium Silicate was 94.87 @ RPM: 350, TEMP: 55, pH: 3.2. The yield was not computed for the Shell Thickness, due to the number of specimens that required cutting for analysis. There were also no results at the variation of 49° for DCDP, due to the temperature being too low to enable the microencapsulation to take place.

3.4.2 Microcapsule Morphology and Shell Thickness

Microcapsule shell thickness

The goal for the shell wall thickness is to be between 140 – 200 nm. It is important that the microcapsules have a specific strength, in order to maintain its structure during the mixing

process. The main application to control this parameter is that of the pH. This was done at several different levels. First, the pH remained constant between 3.68 and 3.67 during trials that controlled the diameter. This allowed the maintaining of a consistent streamlined thickness throughout the multiple trials. Second, the starting pH was varied at 3.7, 3.4 and 3.1 for DCDP. However, as the temperature increased the pH decreased. Therefore, after two hours the pH stabilized at 2.12, 1.95, and 1.81 for the starting pH of 3.7, 3.4, and 3.1, respectively. Similarly, for the sodium silicate synthesis, the starting pH was varied at 3.2, 3.1, and 3.0 and after two hours of heating it decreased to 2.4, 2.3, and 2.2, respectively.

An analysis of the results is given for the DCDP microcapsules. Figure 3.5 (a) illustrates the thickness at three different temperatures. At 49°C, the solution remained an emulsion and no encapsulation took place. However, at temperatures of 52°C and 55°C, the shell thickness remained similar with a slight increase at the higher temperature. Figure 3.5 (b) represents an illustration of the shell thickness at 6 different rpm rates. The shell thickness remained between 130 nm and 470 nm within the rpm range of 250 – 1000 rpm. However, at an rpm rate of 1000, the thickness increased substantially (over 650 nm in thickness). Figure 3.5 (c) represents the variation of the shell thickness at three different pH rates. At a pH of 3.1 and as shown in Figure 3.5, the microcapsule shell thickness is at its strongest point. This supports the assumption that, as the pH is reduced, the shell thickness increased.

For sodium silicate, Figure 3.6 (a) shows a steady increase in shell thickness from 51°C to 55°C. However, after four additional trials at 53°C, there were no microcapsules formed at this temperature. For the rpm variations, as depicted in Figure 3.6 (b), sodium silicate indicates a slight increase in shell thickness at the lower rpm. This is the complete opposite within comparison to DCDP; as DCDP was at its highest thickness at higher rpms. The shell thickness for the pH variation, as shown in Figure 3.6 (c), was at its strongest as the pH increased. As the pH is lowered, the shell wall became nonexistent as no microencapsulation took place. Figure 3.7 (a, b and c) represents the shell wall thickness of a microcapsule after rupturing.

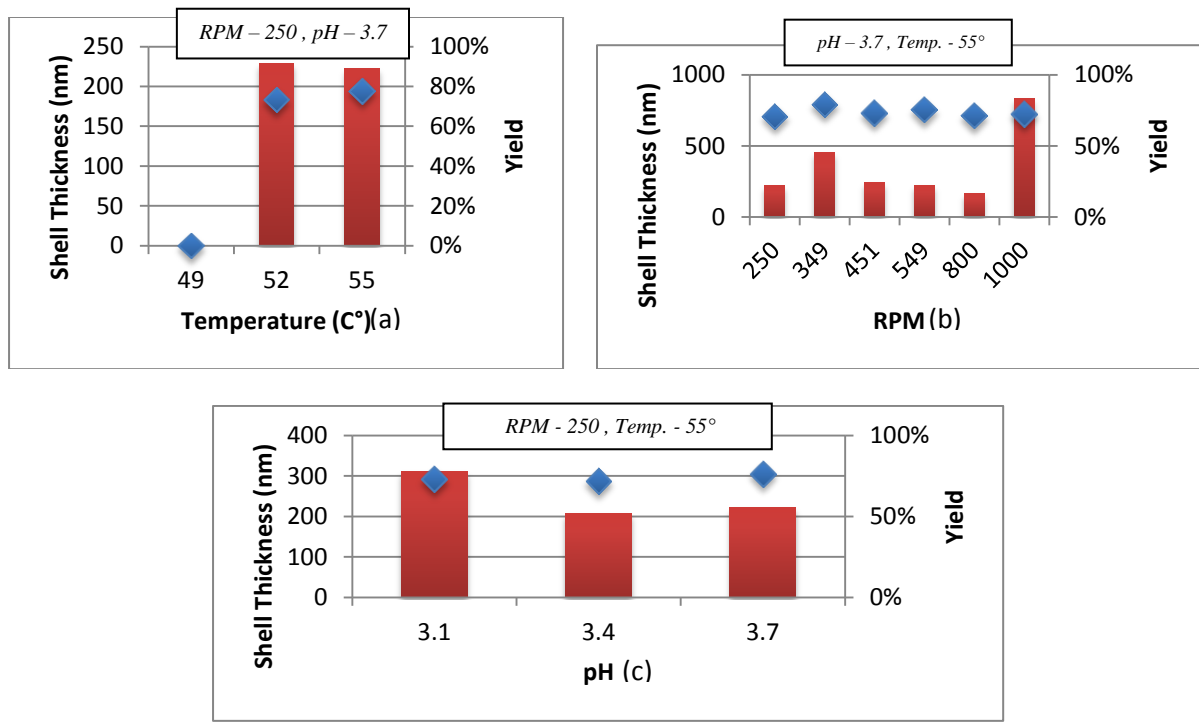


Figure 3.5 DCDP Microcapsule Shell Thickness & Yield vs. (a) Temperature (b) RPM (c) pH

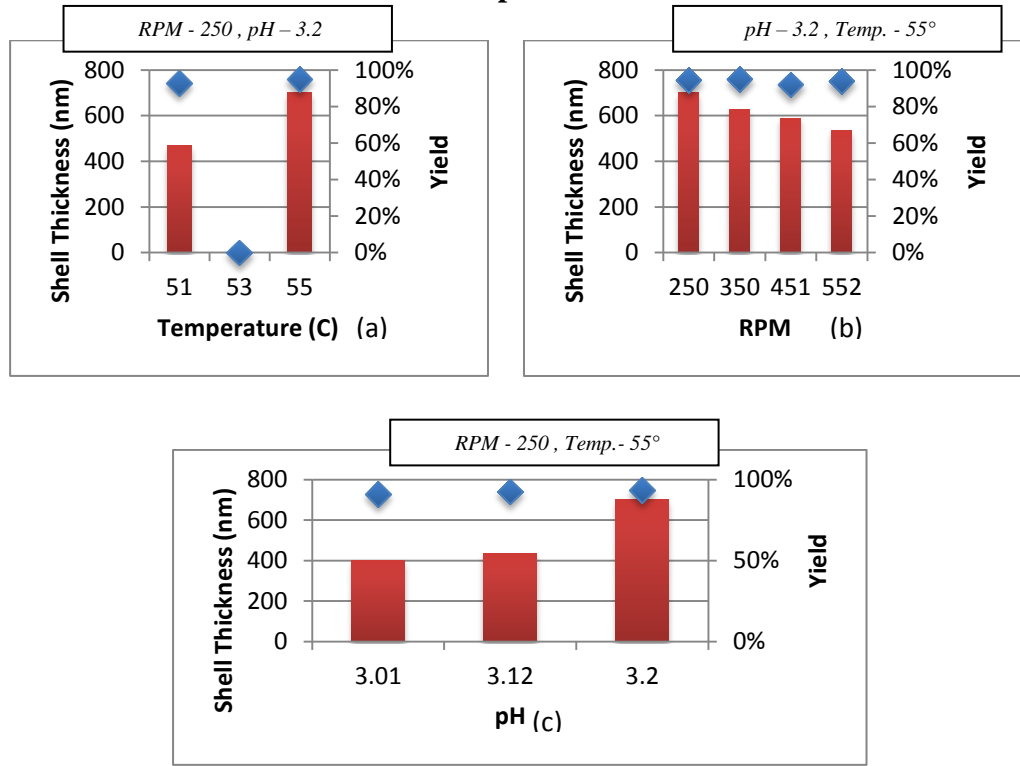


Figure 3.6 Sodium Silicate Microcapsule Shell Thickness & Yield vs. (a) Temperature (b) RPM (c) pH

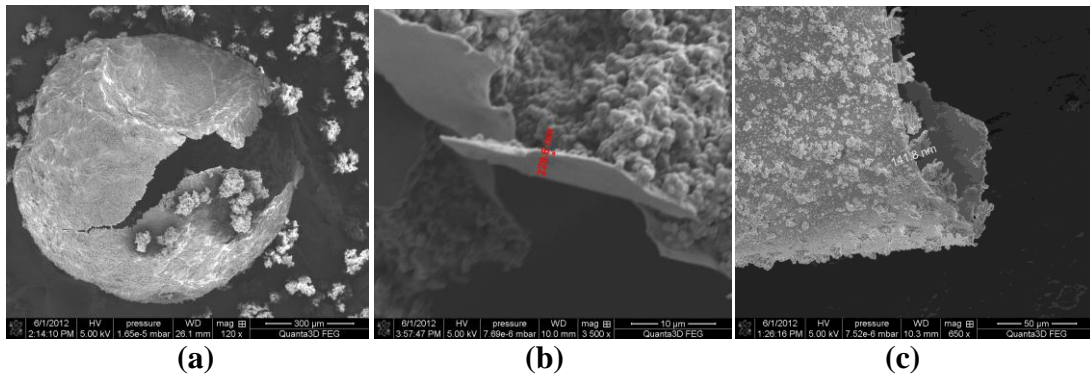
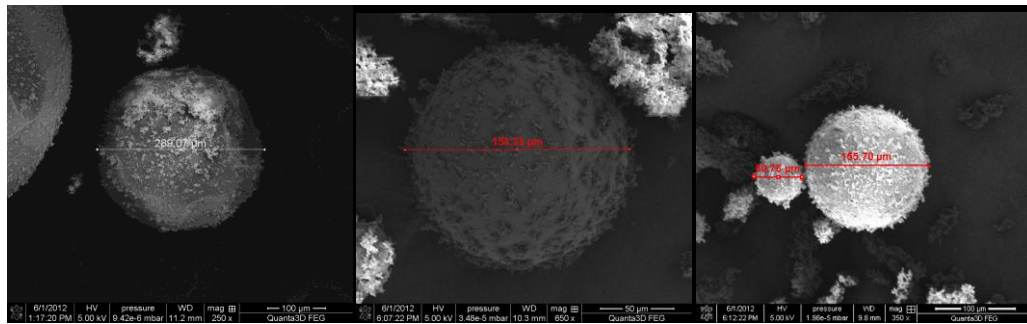


Figure 3.7 Ruptured Micro-capsule with Shell Wall Thickness

Microcapsule surface morphology

During the *in situ* process, water is required for the reaction between urea and formaldehyde to occur. If there were a slight variation with materials, the microcapsules would not produce a smooth porous membrane shell. By ensuring the agitation methods (three bladed shear driver) were consistent, the associated chemical properties would also be consistent. As long as the EMA remains a soluble liquid, the microcapsule wall is developed due to the implementation of the low molecular weight of the EMA while the DCDP interacts with H₂O. When the emulsion of EMA evolves from a solution to a solid phase, this unique phase transition allows the Urea and the Formaldehyde bond, therefore, allowing the microcapsule shell wall to form accordingly. This occurrence provides the smooth wall of the microcapsule itself. By changing the temperature, pH and rpm simultaneously, the morphology substantially changes. With these factors known, the key to the morphology with this experiment is the consistency the synthesis parameters. As shown in Figure 3.8 a, b and c, the morphology of the microcapsule was inconsistent. This was due to the particles not fully attaching themselves to the wall uniformly. This was an important goal to not only streamline this process to provide a smooth morphology, but to also have a strong wall core as well.



(a) (b) (c)
Figure 3.8 Inconsistent Microcapsule Morphology

As depicted in Figure 3.9 (a, b and c), the smoothest and most uniform spherical shape was established at an rpm of 800, pH of 3.7 and a temperature of 55°C. Sodium Silicate developed a morphology that was not consistent with DCDP. Due to the transition of sodium silicate from a liquid to a gel/solid substance, the microcapsules were not uniform in morphology as depicted in Figures 3.10 (a, b and c).

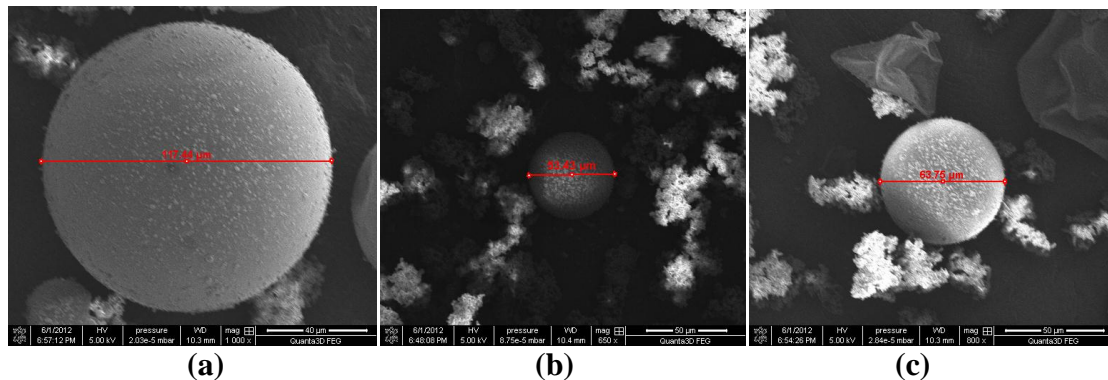


Figure 3.9 Representation of Smooth Microcapsule Morphology

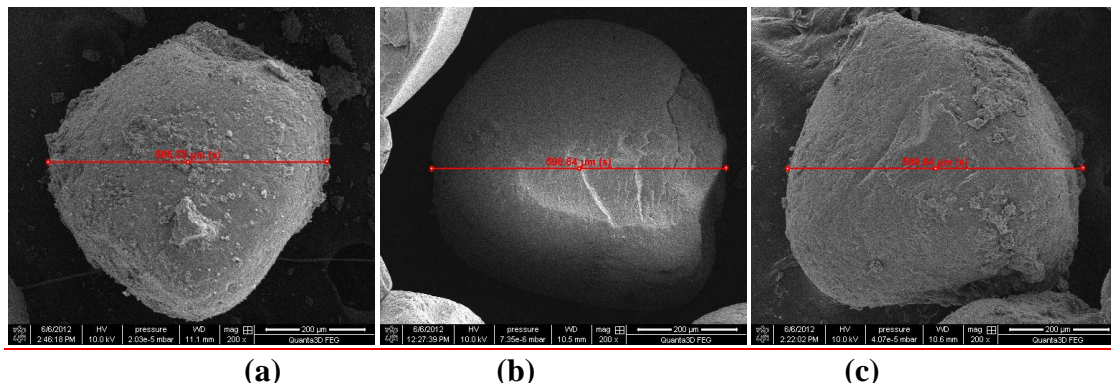
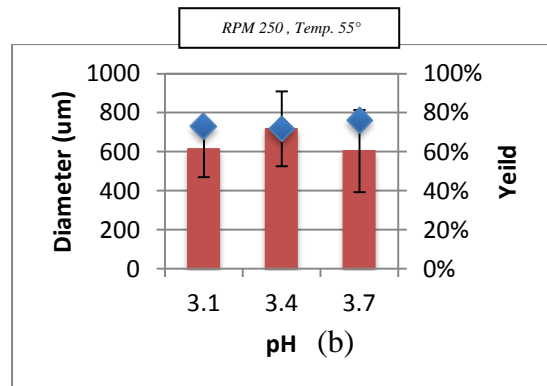
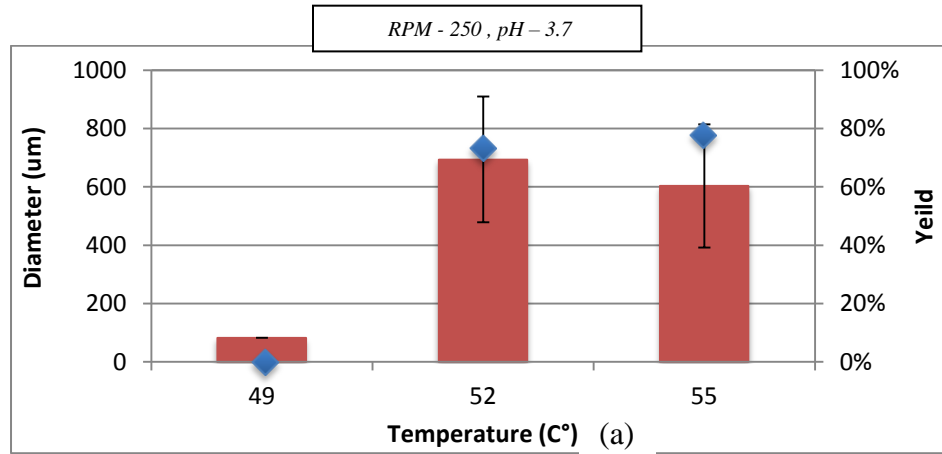


Figure 3.10 Sodium Silicate Non-Uniform Microcapsules

3.4.3 Controlling Diameter and Size

There is evidence of a linear (log/log) relationship between the agitation rate and the average diameter as shown in Figure 3.11 (c). An important factor in this occurrence is the shear rate during agitation and the droplet size of the solution while added. When the agitation rate is between 250 – 1000 rpm, the microcapsule average size is between 50 μm – 800 μm . In Figure 3.11 (a), the DCDP microcapsule diameter is at the greatest diameter at 52°C. In retrospect to pH, as depicted in Figure 3.11 (b), a pH of 3.4 resulted in the largest microcapsule generation at 55°C. At multiple rpm variations, as seen in Figure 3.11 (c), there was a decrease in microcapsule diameter as the rpm rate began at 250 and was increased to 1000 rpm. The variation of diameter size was consistent between 800 and 1000 rpm, with all sizes averaging below 100 μm .



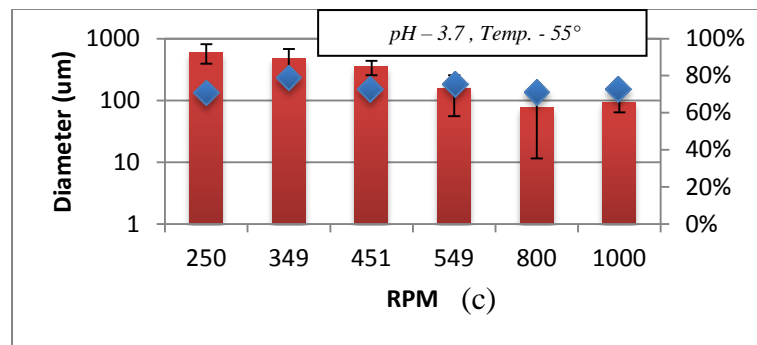


Figure 3.11 DCDP Microcapsule Diameter vs. (a) Temperature (b) pH (c) RPM

The diameter also changed substantially for sodium silicate as parameters were altered. Figure 3.12 (a) presents an illustration of the diameter change at three different temperatures. From this figure, it is shown that a temperature of 51°C at an rpm rate of 250 and a pH of 3.2, will provide the largest microcapsule diameter. The best pH to utilize for Sodium Silicate, was at a pH of 3.2 as illustrated in Figure 3.12 (b). The diameter of the microcapsules remained constant, as depicted in Figure 3.12 (c). This is due to the consistency of the gel-like/solid solution, compared to the aqueous solution of DCDP.

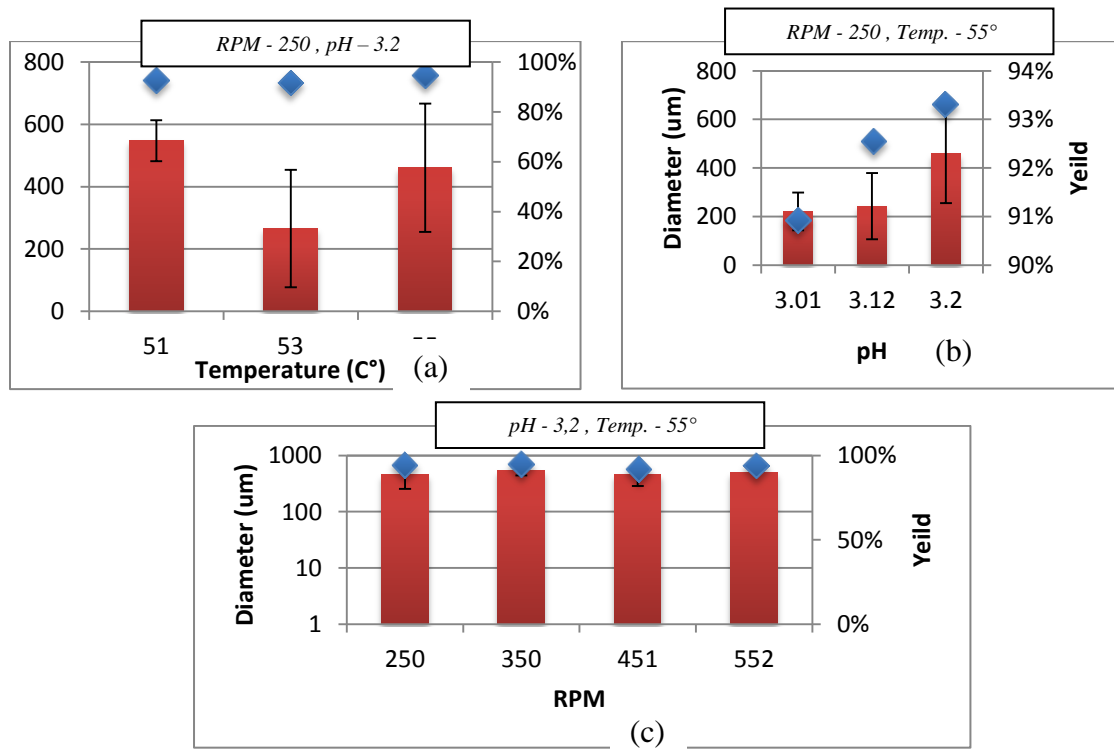


Figure 3.12 Sodium Silicate Microcapsule Diameter vs. (a) Temperature (b) pH (c) RPM

3.5 CONCLUSIONS

The results from the data presented various amounts of information. In Figure 3.5a, DCDP was varied at three different temperatures (55° , 52° and 49°) at a constant rpm of 250 and a pH of 3.7 in order to assess the microcapsule shell thickness. From this figure, the temperature of 52° provided the largest shell thickness at 239 nm. At 49° , no microcapsules were generated were not generated most likely due to the molecular weight of the pre-polymers not reaching the requirement for encapsulation. In reference to Figure 3.5b, the rpm was varied of 6 different levels while keeping the temperature at 55° and a pH of 3.7.

There is a linear log relationship with agitation and diameter. As the agitation increased, the microcapsule shell thickness became smaller. However, at an rpm of 1000, the shell thickness almost tripled. This was most likely due to particles forming and bonding together at a much faster rate. Figure 3.6c represents the last parameter varied to analysis shell thickness. As the pH decreased, the shell thickness increased as well. These results were expected from previous literature review and experimental analysis by other Universities as Doctors. Sodium Silicate (SS) possessed different results in relation to shell thickness. Unlike DCDP, Sodium Silicate shell thickness was almost twice the amount of DCDP. This was due to Sodium Silicate (SS) being transformed into a gel like solution prior to micro-encapsulation.

This gel solution made the compound much easier to encapsulate, as well as build a much stronger shell wall. For example, Figure 3.6a represents a variation of different temperatures in order to evaluate the shell thickness. 51° and 55° provided an average shell thickness of between 480 and 700 nm, whereas the shell thickness of 53° could not be determined. Sodium Silicate also produced interesting results for the pH variation in Figure 3.6c. As the pH increased, the shell thickness increases. In relation to the agitation analysis, as the agitation rate increased, the shell thickness became smaller. Controlling the capsules morphology was extremely challenging. For example, during the experimental analysis, it was confirmed and determined that temperature possesses a direct relationship with the pH for both Sodium Silicate and DCDP. As the temperature increased during the trials, the pH decreased.

Variations of these parameters resulted in a non uniform morphology. Figure 3.8 is an representation of the parameters of pH and Temp being varied. Figure 3.9 however, is a direct result of those parameters being consistent. As pH and Temp was stabilized and consistent, as indicated in Figure 3.10, a uniform smooth micro-capsule morphology was produced. Due to the

performance factors of Sodium Silicate (High pH), this parameter was difficult to stabilize a replicate consistently. For both experiments, the pH was a challenging factor. For DCDP, the pH was stabilized at 3.5 during the beginning of the experiment.

As the temperature began to rise from room temperature to approximately 55°, the pH was lowered from 3.5 to approximately 2.35. For Sodium Silicate, the pH was stabilized at 3.2. As the temperature rose, the pH dropped and stabilized at 2.3-2.4 after two hours. Temperature has a direct impact on the forming of the wall and core during the interfacial polymerization phase. Although the ability to maintain this consistency with the pH is important and essential, agitation rate is the key factor that controls the microcapsule capsule diameter size. As the agitation rate is increased, the microcapsule diameter size will decrease. If the agitation rate decreases, the microcapsules will become larger.

Sodium silicate, however, was not consistent with the normal parameter matrix, due to its alkaline nature. As the agitation rate increased, the size remained normal and consistent. This was due to the attempt to stabilize the Sodium Silicate solution for the micro-encapsulation procedure of Urea-Formaldehyde. Nevertheless, both Sodium Silicate and DCDP trials were successful in meeting the overall objective of this thesis, which was to control the performance parameters of the two self-healing methods. Although successful, there is much more research within this area that needs to be conducted.

3.6 REFERENCES

Brown, E.N., M.R. Kessler, N.R. Sottos, and S.R. White. In situ poly(urea-formaldehyde) microencapsulation of dicyclopentadiene. *Journal of Microencapsulation*, Vol. 20, No. 6, 2003, pp. 719-730.

Brown^a, E.N., S.R. White, and N.R. Sottos. Retardation and repair of fatigue cracks in a microcapsule toughened epoxy composite-Part I: Manual infiltration. *Composites Science and Technology*, Vol. 65, Is. 15-16, 2005, pp. 2466-2473.

Brown^b, E.N., S.R. White, and N.R. Sottos. Retardation and repair of fatigue cracks in a microcapsule toughened epoxy composite-Part II: In situ self-healing. *Composites Science and Technology*, Vol. 65, Is. 15-16, 2005, pp. 2474-2480.

Greenwood, N. N. and A. Earnshaw. *Chemistry of the Elements* (2nd ed.). Butterworth–Heinemann, 1997.

Jinglei Yang, Michael W. Keller, Jeffery S. Moore, Scott R. White, and Nancy R. Sottos, Microencapsulation of Isocyanates for Self-Healing Polymers, *Macromolecules*, 2008

Kessler, M.R., N.R. Sottos, and S.R. White. Self-healing structural composite materials. *Composites: Part A*, Vol. 34, 2003 pp 743-753

Nonat, A. Structure and Stoichiometry of C-S-H. *Cement and Concrete Research*, Vol. 34, Is. 9, 2004, pp. 1521-1528.

Tseng, Y.H, M.H. Fang, P.S. Tsai, and Y.M. Yang. Preparation of microencapsulated phase-change materials (MCPCMS) by means of interfacial polycondensation. *Journal Microencapsulation*. Vol. 22, No.1, 2005, pp. 37-46.

White, S.R., N.R. Sottos, P.H. Geubelle, J.S. Moore, M.R. Kessler, S.R. Sriram, E.N. Brown, and S. Viswanathan. Autonomic healing of polymer composites. *Nature*, Vol. 409, 2001, pp. 794-797.

CHAPTER 4

SUMMARY AND CONCLUSIONS

The comparison and contrast methods between the two encapsulation procedures were extremely complex and challenging. DCDP and Sodium Silicate, both independently, pose completely different performance parameters as self-healing methods. DCDP remains a liquid throughout the encapsulation process and its pH and consistency remains the same. Sodium Silicates composition posed a requirement to be changed from a liquid to a gel. This was due to its highly alkaline nature and response to the Urea – Formaldehyde microencapsulation process itself. The handling of DCDP was a challenge due to its toxicity. Before handling these healing agents and its disposal, many safeguards must be met by the user.

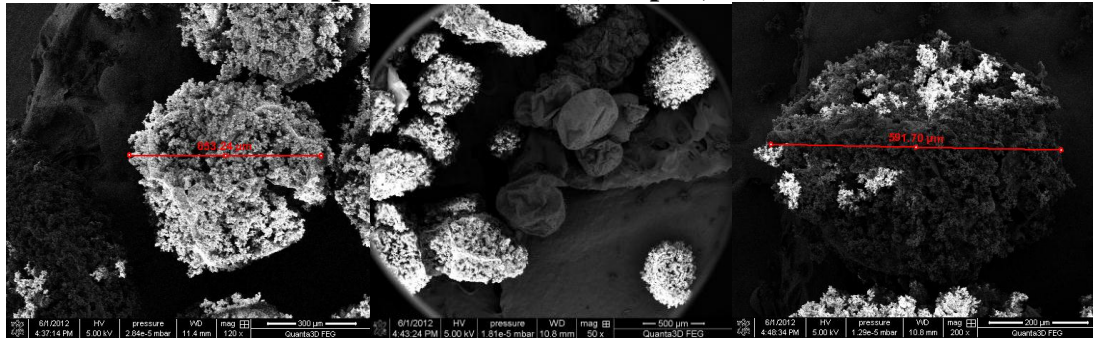
4.1 FUTURE WORK

DCDP is a healing agent that requires the completion of a matrix in order to be successful. More research must be instituted in testing the different parameters along with the matrix itself in concrete applications. The Urea Formaldehyde method of Sodium Silicate has never been tested. The next step is to apply these microcapsules to a concrete mix design and evaluate and analysis its effectiveness. The shell thickness and strength of these capsules have not been tested in actual concrete structures. The effectiveness of different size self-healing microcapsules within a concrete sample still needs to be tested. Furthermore, it is also not known how and in what capacity self-healing will assist/heal large concrete structures.

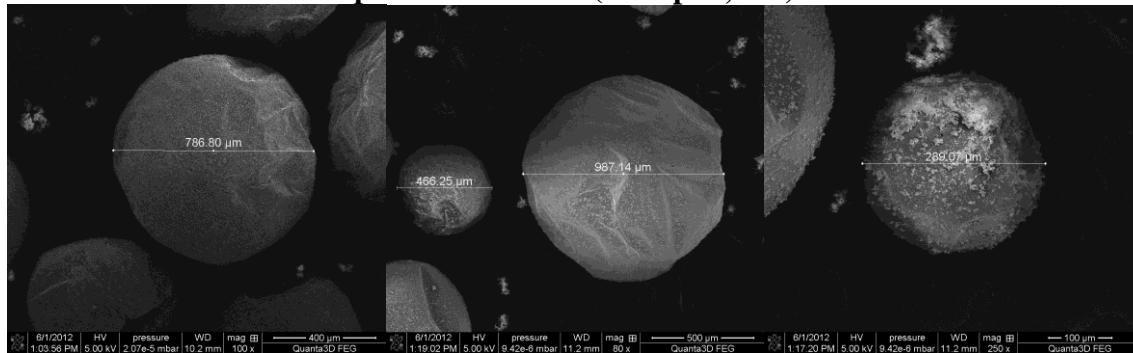
Appendix: SEM MICROCAPSULE ANALYSIS

DCDP ANALYSIS

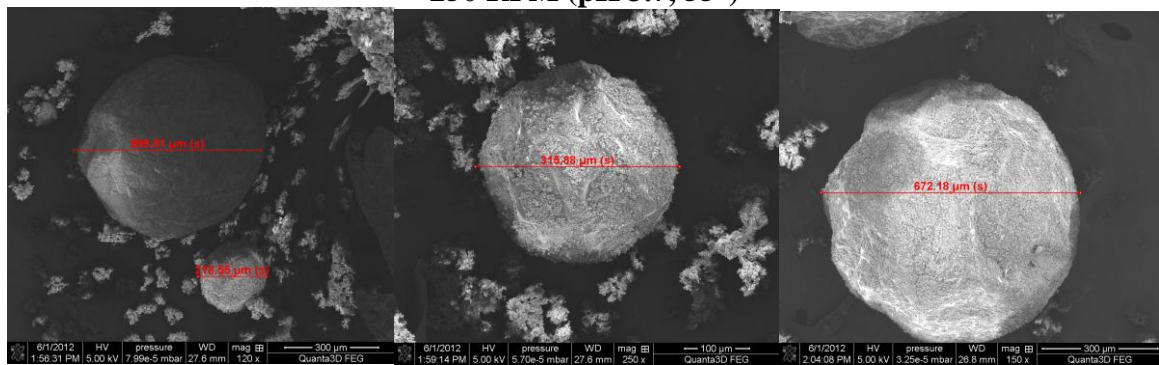
pH 3.1 Variation (250 rpm., 55°)



pH 3.4 Variation (250 rpm., 55°)

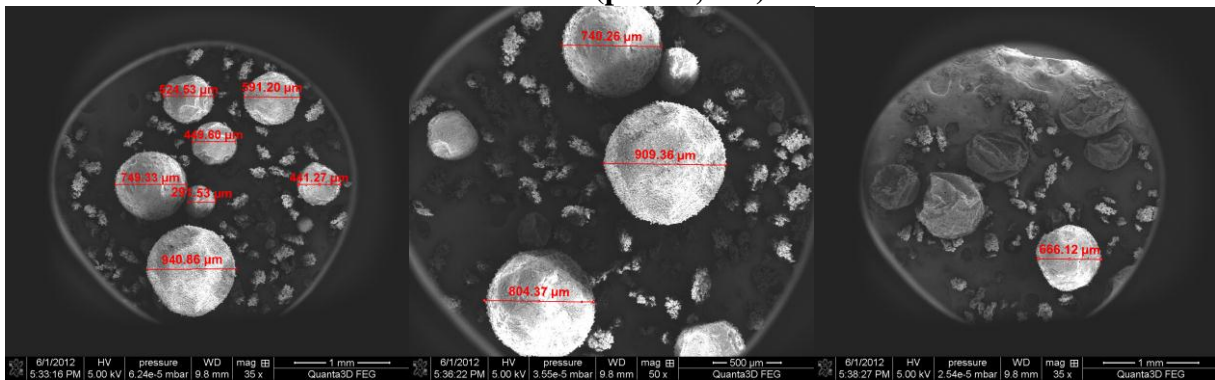


250 RPM (pH 3.7, 55°)

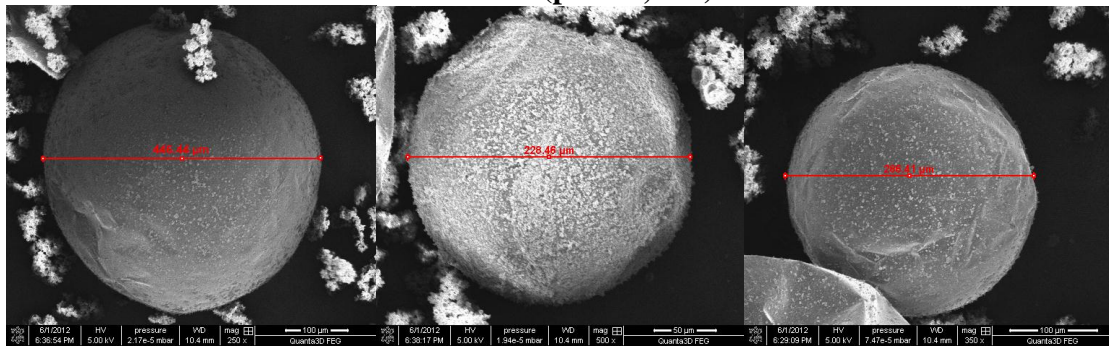


\

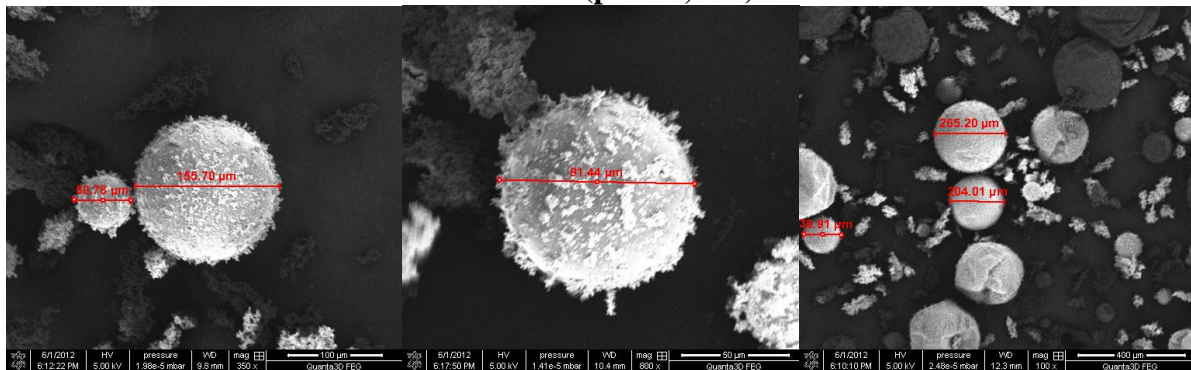
349 RPM (pH 3.7, 55°)



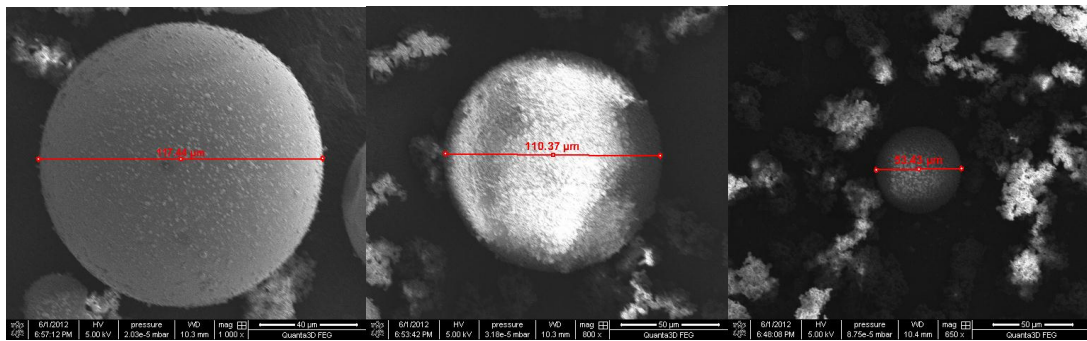
451 RPM (pH 3.7, 55°)



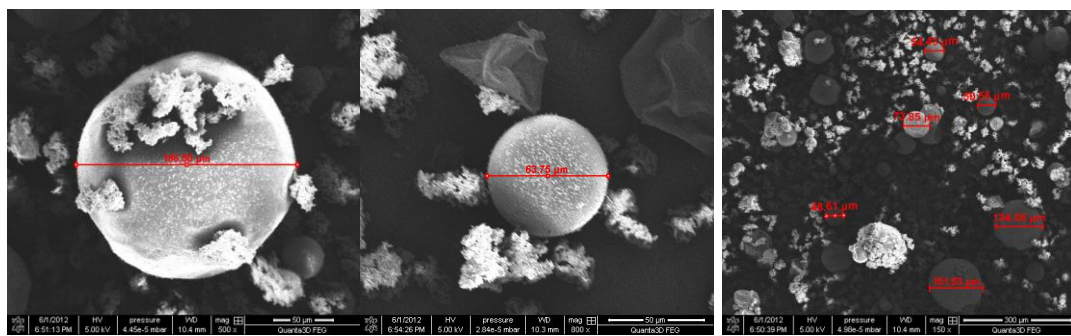
549 RPM (pH 3.7, 55°)



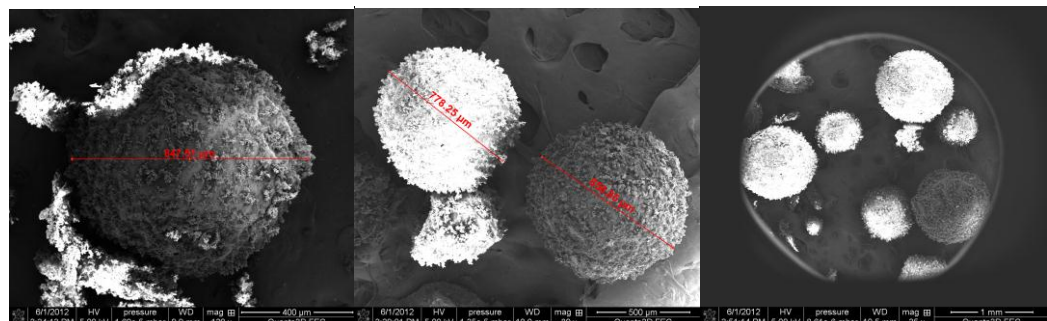
RPM 800 (pH 3.7, 55°)



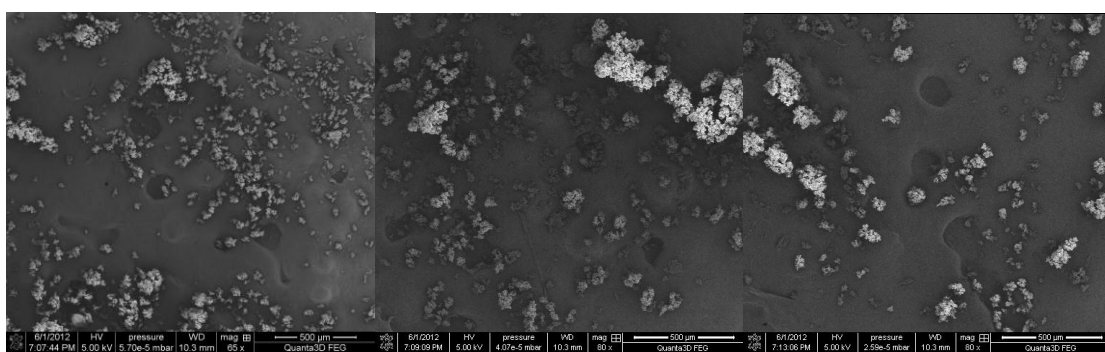
RPM 1000 (pH 3.7, 55°)



TEMP. 52° (pH 3.7, RPM 250)

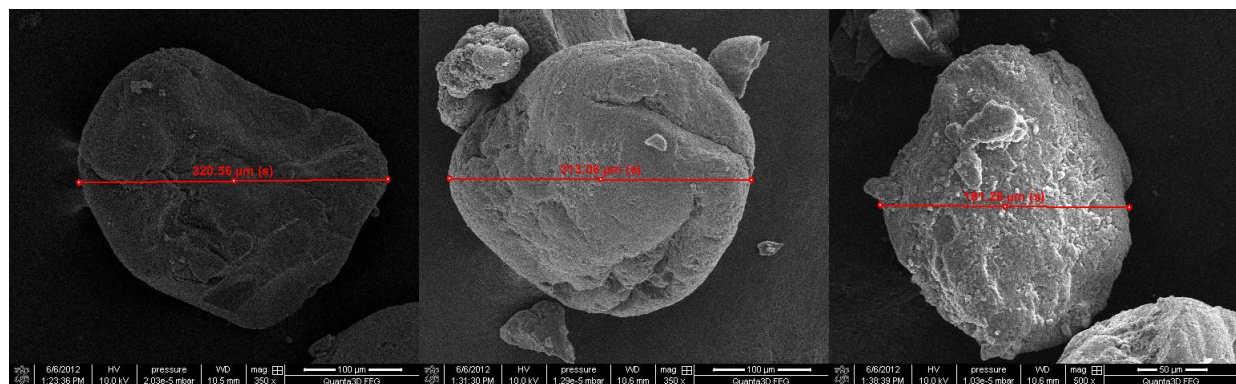


TEMP. 49° (pH 3.7, RPM 250)

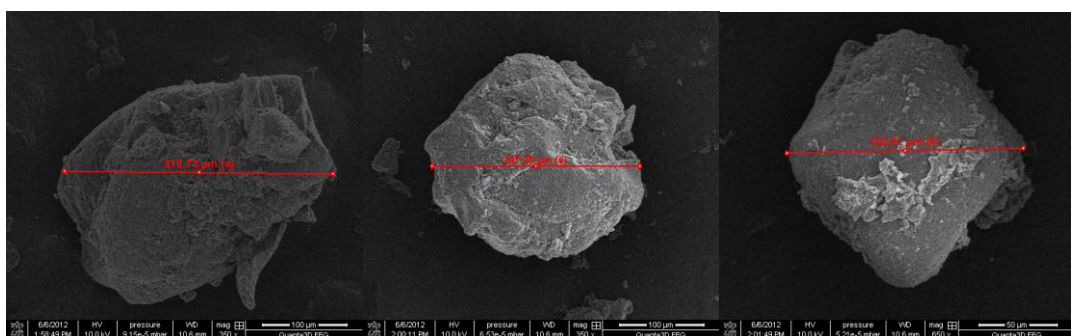


SODIUM SILICATE

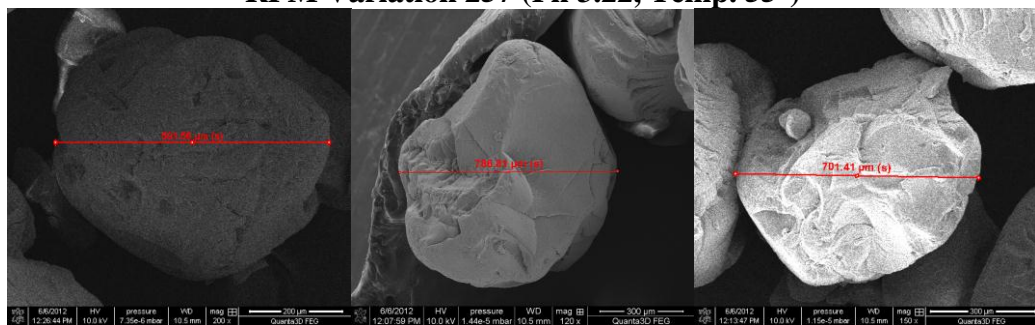
pH Variation 3.12 (251 RPM, Temp. 55°)



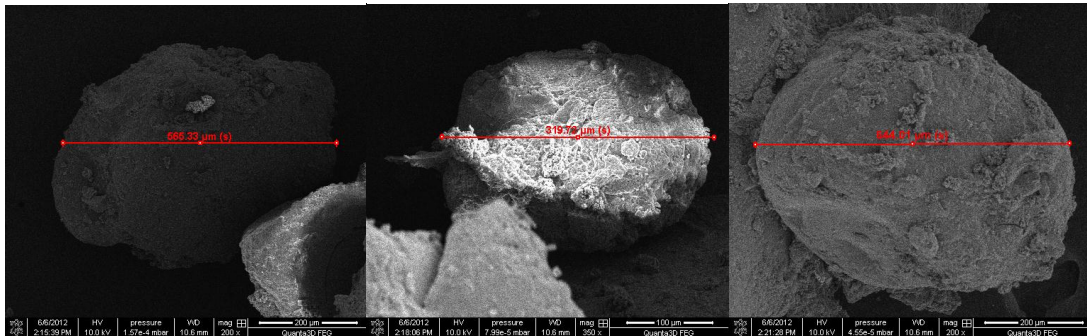
pH Variation 3.12 (251 RPM, Temp. 55°)



RPM Variation 257 (Ph 3.22, Temp. 55°)



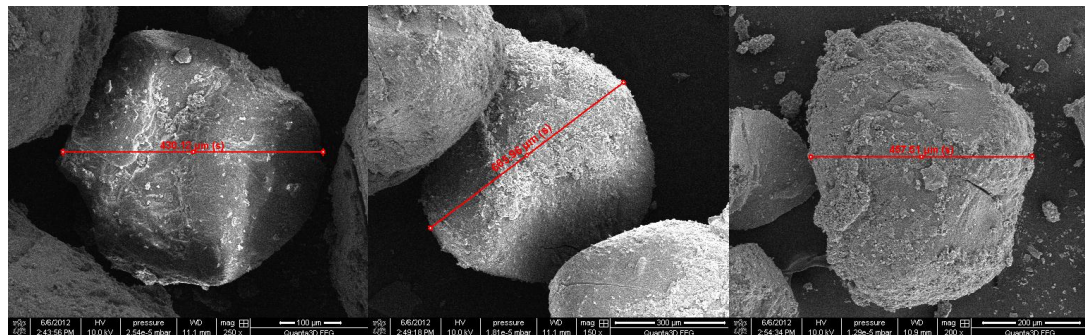
RPM Variation 352 (pH 3.22, Temp. 55°)



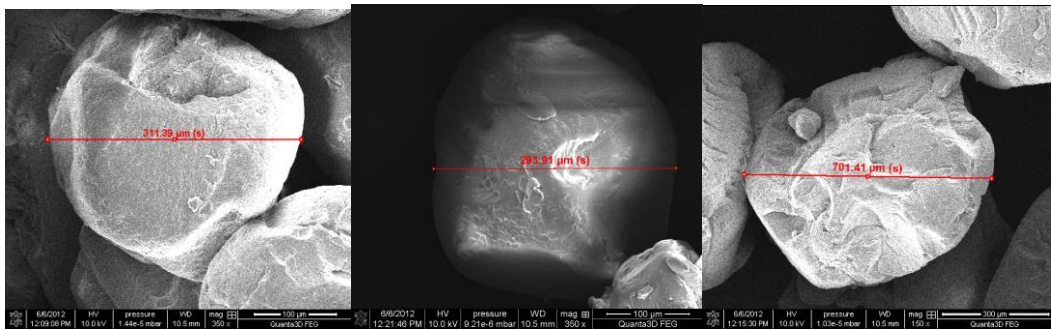
RPM Variation 454 (pH 3.22, Temp. 55°)



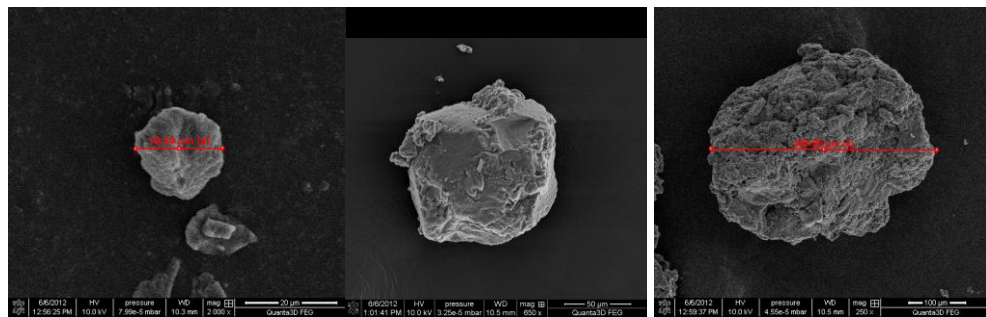
RPM Variation 551 (pH 3.21, Temp. 55°)



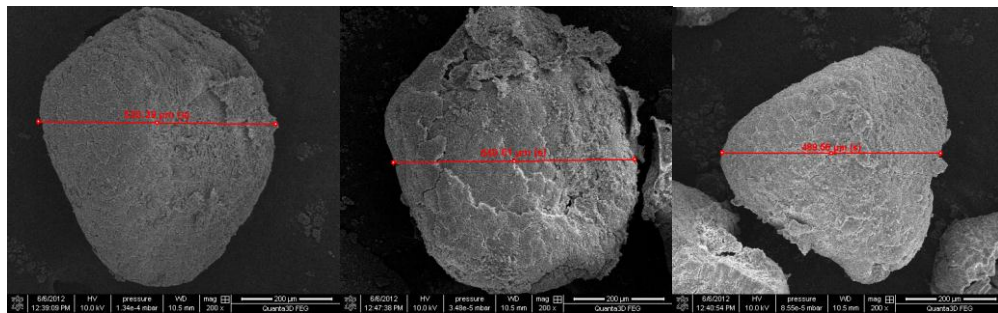
TEMP. Variation 55° (pH 3.23, RPM 255)



TEMP. Variation 53° (pH 3.23, RPM 255)



TEMP. Variation 51° (pH 3.23, RPM 255)



VITA

LCDR James Gilford III was born in Beaumont, Texas on November 25, 1977. After graduating from Central high school in Beaumont as a Texas Scholar, he chose to attend Prairie View A&M University. During his tenure at Prairie View, he pledged and joined elite organizations such as; Alpha Phi Alpha Fraternity, Inc., Alpha Phi Omega International Service Organization, and Prince Hall Masons. On December 19, 2001 James Gilford III was presented with a Bachelor of Science Degree in Civil Engineering.

After graduating college LCDR Gilford began his journey to become a Naval Officer by attending Officer Candidate School (OCS) in March 2002 in Pensacola, FL. LCDR Gilford was commissioned as a Naval Officer on August 4, 2002. He was then selected as one of the few to participate in the ‘new’ Introductory Flight Syllabus Program (IFS), where he learned the basics of flying. After completing the IFS program in Milton, FL., LCDR Gilford reported back to Pensacola, FL. to begin Aviation Preflight Indoctrination (API) in November 2002. Once API was complete, he then began his primary syllabus by flying the T-34 at NAS Corpus Christi, in Corpus Christi, TX.

In November of 2003, he continued his training to become a Naval Aviator by entering the helicopter pipeline at NAS Whiting Field, in Milton, FL. He was winged and designated a Naval Aviator August 4th, 2004. LCDR Gilford was assigned to the Fleet Replacement Squadron (FRS), Helicopter Antisubmarine Squadron Light FOUR ZERO (HSL-40) where he completed training in the SH-60B Seahawk. Immediately following his completion of the fleet replacement pilot syllabus, he received orders to his first operational squadron, HSL-42, in Mayport, Florida. He served as Ground Safety officer, Ground Training Officer, and Volunteer Coordinator before joining Detachment Three. As a Naval Aviator he has flown over 900 flight hours, completed over 50 missions in theatre (Iraq and Horn of Africa), and over 2,000 landings on over 18 different platforms. LCDR Gilford is the proud father of Katelyn T. Gilford, who was born on January 10, 2007, and has been a light in his path since her birth. He enjoys the following: competitive shooting, hunting, fishing, camping, water sports, and horse back riding.

After serving his country in the air, on January 22, 2008 James decided to become a member of a unique organization, the Civil Engineering Corps. Before his lateral transfer board selection in October of 2008, he was granted the opportunity from his squadron to be sent TAD

to the PWD at NAS Jacksonville for 3 months. Relying on his previous construction knowledge, he successfully resolved multiple unforeseen site conditions on the renovation of temporary administrative spaces supporting the \$16M BRAC Engineering Ops Center. He worked quickly and efficiently to develop engineering solutions that fully supported active operations without any adverse impacts. In March of 2008, James volunteered and received orders for an IA assignment for NPDB-5 in Camp Bucca, Iraq. During his tour he served as Alpha Company Commander as well as a Compound OIC. LCDR Gilford returned from a successful 12 month IA tour in April of 2009, and began CECOS in May of 2009. He checked in to NMCB-7 in September of 2009. While at NMCB-7 he served as Airfield Damage Officer in charge as well as the ALFA Company Commander. He also earned his Seabee Combat Warfare Certification while attached to Battalion. After receiving his Masters in Engineering Science from Louisiana State University, he plans to move to Washington, D.C. in continuing to serve his country as a Civil Engineer.